

# Recent multi-decadal Southern Ocean surface cooling unlikely caused by Southern Annular Mode trends

Yue Dong<sup>1</sup>, Lorenzo M Polvani<sup>1</sup>, and David Bonan<sup>2</sup>

<sup>1</sup>Columbia University

<sup>2</sup>California Institute of Technology

September 11, 2023

## Abstract

Over recent decades, the Southern Ocean (SO) has experienced multi-decadal surface cooling despite global warming. Earlier studies have proposed that recent SO cooling has been caused by the strengthening of surface westerlies associated with a positive trend of the Southern Annular Mode (SAM) forced by ozone depletion. Here we revisit this hypothesis by examining the relationships between the SAM, zonal winds and SO sea-surface temperature (SST). Using a low-frequency component analysis, we show that while positive SAM anomalies can induce SST cooling as previously found, this seasonal-to-interannual modulation makes only a small contribution to the observed long-term SO cooling. Global climate models well capture the observed interannual SAM-SST relationship, and yet generally fail to simulate the observed multi-decadal SO cooling. The forced SAM trend in recent decades is thus unlikely the main cause of the observed SO cooling, pointing to a limited role of the Antarctic ozone hole.

1       **Recent multi-decadal Southern Ocean surface cooling**  
2       **unlikely caused by Southern Annular Mode trends**

3       **Yue Dong<sup>1,2</sup>, Lorenzo M. Polvani<sup>1,3</sup>, David B. Bonan<sup>4</sup>**

4                   <sup>1</sup>Lamont-Doherty Earth Observatory, Columbia University, Palisades, NY, USA

5                   <sup>2</sup>Cooperative Programs for the Advancement of Earth System Science, University Corporation for

6                                   Atmospheric Research, Boulder, CO, USA

7                   <sup>3</sup>Department of Applied Physics and Applied Mathematics, Columbia University, New York, NY, USA

8                   <sup>3</sup>Environmental Science and Engineering, California Institute of Technology, Pasadena, CA, USA

9       **Key Points:**

- 10       • Austral summer SAM variability affects Southern Ocean SST only on seasonal to  
11       interannual timescales
- 12       • The short-term SAM-SST relationship makes little contribution to the observed  
13       multi-decadal Southern Ocean SST trends
- 14       • GCMs capture the observed seasonal SAM-SST relationship and yet fail to sim-  
15       ulate the observed long-term SO cooling

---

Corresponding author: Yue Dong, [dongyueatmos@gmail.com](mailto:dongyueatmos@gmail.com)

## Abstract

Over recent decades, the Southern Ocean (SO) has experienced multi-decadal surface cooling despite global warming. Earlier studies have proposed that recent SO cooling has been caused by the strengthening of surface westerlies associated with a positive trend of the Southern Annular Mode (SAM) forced by ozone depletion. Here we revisit this hypothesis by examining the relationships between the SAM, zonal winds and SO sea-surface temperature (SST). Using a low-frequency component analysis, we show that while positive SAM anomalies can induce SST cooling as previously found, this seasonal-to-interannual modulation makes only a small contribution to the observed long-term SO cooling. Global climate models well capture the observed interannual SAM-SST relationship, and yet generally fail to simulate the observed multi-decadal SO cooling. The forced SAM trend in recent decades is thus unlikely the main cause of the observed SO cooling, pointing to a limited role of the Antarctic ozone hole.

## Plain Language Summary

Under increased greenhouse gases, the Southern Ocean sea-surface temperatures have cooled over the recent several decades. The cause of Southern Ocean cooling remains a puzzling feature of recent climate change. Earlier studies have proposed that this multi-decadal cooling in the Southern Ocean has arisen in part from the strengthening of surface winds associated with a positive trend in a mode of climate variability known as the Southern Annular Mode (SAM). Here we employ a new statistical method to examine this proposed relationship in both observations and climate models. We found that SAM variability only changes Southern Ocean surface temperature on short-term timescales and makes little contribution to observed long-term trends. Our results thus suggest the SAM trend, via the strengthening of circumpolar westerlies, is unlikely the main cause of the observed long-term Southern Ocean cooling.

## 1 Introduction

Unlike the Arctic, the Southern Ocean has experienced substantial cooling in recent decades, following an earlier warming period from the 1950s to 1980s (Fig. 1a). This multi-decadal surface cooling over the Southern Ocean has been accompanied by anomalous surface freshening, sub-surface warming, and an expansion of sea ice around Antarctica (Fan et al., 2014; De Lavergne et al., 2014; Armour et al., 2016; Parkinson, 2019; Roach et al., 2020), all of which remain puzzling features of the observed climate change in the Southern Hemisphere. Apart from its local impacts, Southern Ocean surface cooling has been found to have remote effects on the pattern of tropical surface warming (Hwang et al., 2017; Dong, Armour, et al., 2022; Kim et al., 2022), tropical atmospheric circulation (Kang et al., 2020, 2023), and estimates of the global warming rate and climate sensitivity (Dong, Pauling, et al., 2022).

Despite its broad impacts on both the local and global climate, the observed Southern Ocean SST trend remains poorly simulated by global climate models (GCMs) (Fig. 1c). GCM initial-condition large ensembles (Deser et al., 2020) generally produce too strong SO surface warming over recent decades (Wills et al., 2022), along with too weak surface freshening and positive trends in Antarctic sea-ice extent (Roach et al., 2020). These model deficiencies over the historical period thus call into question the reliability of model projections of future Antarctic climate change.

Several hypotheses have been put forward to explain the observed multi-decadal SO cooling, including SO natural variability driven by ocean convection (Polvani & Smith, 2013; Latif et al., 2013; Cabré et al., 2017; Zhang et al., 2019), freshwater input from Antarctic ice-sheet melt (Rye et al., 2020; Pauling et al., 2016; Bintanja et al., 2013; Purich et al., 2018; Purich & England, 2023) or from increased equatorward sea-ice melt (Haumann

et al., 2020). These hypotheses, however, are mostly built on modeling evidence, and are thus potentially subject to model biases. An alternative hypothesis is that the observed SO cooling trends may be driven by trends in surface westerlies via the Southern Annular Mode (SAM) through northward Ekman transport (Hall & Visbeck, 2002; Lefebvre et al., 2004; Gupta & England, 2006; Ferreira et al., 2015). It has been robustly observed that the surface westerlies have strengthened and shifted poleward, associated with the positive trend in the austral-summer (DJF) SAM over the second half of the 20th century (Thompson & Solomon, 2002; G. J. Marshall, 2003) (also Fig. 1b). This trend in SAM has been in large part attributed to stratospheric ozone depletion (Polvani et al., 2011; Previdi & Polvani, 2014; Banerjee et al., 2020). The observed SAM trend is generally well captured in GCM simulations (Fig. 1d) (Waugh et al., 2020).

To link SST variability to SAM variability, Doddridge and Marshall (2017) carried out an observational study and reported a robust interannual relationship between the SAM and SO SST. Their results show that positive SAM anomalies in the austral summer lead to anomalous cold SST persisting to the following autumn, suggesting a possible contribution of ozone depletion to SO cooling. On the modeling side, the SAM-SST connection on multi-decadal time scales was supported by idealized model simulations with abrupt SAM or ozone forcing (e.g., Ferreira et al., 2015; Kostov et al., 2018; Seviour et al., 2016). Early “step-like” forcing experiments showed a two-time-scale feature of the SO SST response to wind/SAM anomalies – a fast time-scale SST cooling response driven by the northward Ekman transport of surface waters and a slow time-scale SST warming response driven by the upwelling of warmer waters from below. Although a comprehensive study of such idealized experiments showed a very weak relationship between SAM and SST cooling on decadal time scales (Seviour et al., 2019), the appeal of a simple physical mechanism, the observed interannual modulation of SO SST by the SAM – and thus the Antarctic ozone hole – remains popular as a potential explanation of the multi-decadal cooling trends in the SO (Hartmann, 2022).

On the other hand, the causal relationship between SO SST trends and SAM/wind trends is at odds with several studies which have suggested that stratospheric ozone depletion causes surface *warming*, not cooling, on multi-decadal time scale. Unlike the idealized abrupt-forcing simulations that show a “fast” SO cooling response, GCM simulations with realistic transient or time-averaged ozone forcing robustly simulate a SO warming response along with Antarctic sea-ice melting (Sigmond & Fyfe, 2014; Bitz & Polvani, 2012; Smith et al., 2012; Landrum et al., 2017). Additionally, a recent study by Polvani et al. (2021) re-examined the relationship between the SAM and Antarctic sea-ice extent (SIE) in observations and GCMs. They found that the interannual SAM modulation of Antarctic SIE only explains a small fraction of the year-to-year SIE variability, and thus does not account for multi-decadal SIE trends. These studies collectively suggest that SAM variability, associated with the ozone hole, is unlikely to be the main driver of the observed long-term trends in SO SST and Antarctic SIE, contradicting the conclusion of the idealized modeling studies.

Motivated by these discrepancies in previous findings, we aim to address two questions in this study: (i) Can GCMs simulate the observed interannual relationship between the SAM and SO SST? (ii) To what extent does the interannual SAM modulation of SO SST contribute to the multi-decadal cooling trends in observations?

## 2 Interannual SAM modulation of Southern Ocean SST

In this section, we first repeat the analysis in Doddridge and Marshall (2017) (hereafter “DM2017”) and Polvani et al. (2021) to re-examine the interannual SAM-SST relationship in both observations and GCMs. By comparing the results between observations and models, we assess whether model biases in long-term SO SST trends stem in part from model biases in the short-term SAM-SST modulation.

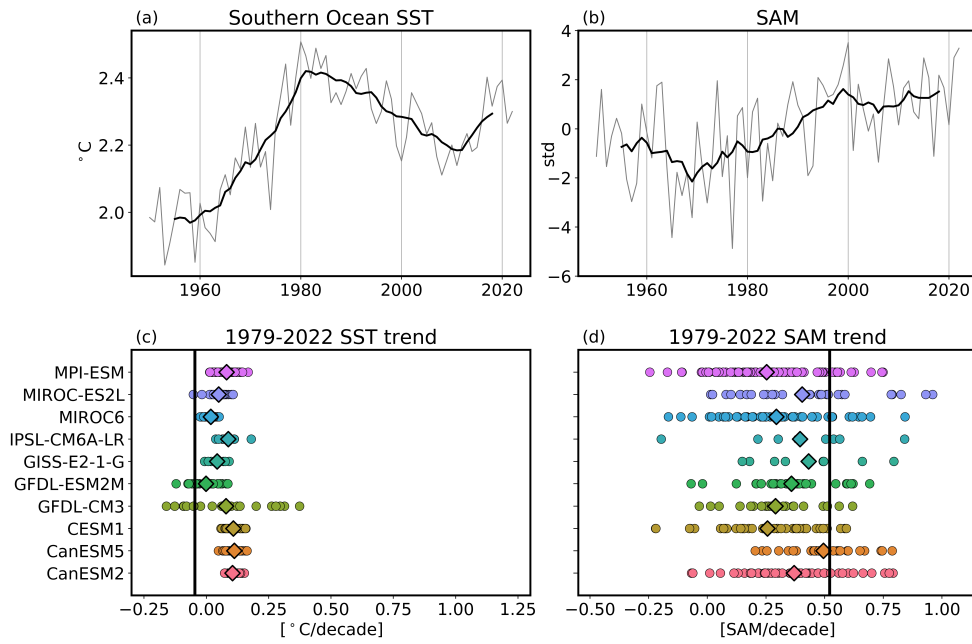


**Figure 1.** Observed and modeled Southern Ocean SST and SAM. (a – b) the observed annual-mean Southern Ocean SST and the DJF SAM index over 1950–2022. Black thicker lines denote 10-year running means. (c-d) the Southern Ocean SST trends and the SAM trend over 1979–2022 in observations (black line) and model large-ensembles. Circles denote each individual ensemble member; diamonds denote ensemble mean.

116

## 2.1 Data

117

118

119

120

121

122

123

124

125

126

127

128

For observations, we use SST from the NOAA Extended Reconstruction Sea Surface Temperature version 5 (ERSSTv5) dataset (Huang et al., 2017) and sea-level pressure (SLP) from the ERA5 Reanalysis dataset (Hersbach et al., 2020), both over the period of 1950–2022. For models, we use SST and SLP from 10 CMIP5 and CMIP6 models, including 5 models participated in multi-model large-ensemble project (Deser et al., 2020) and 5 CMIP6 models that have large ensembles (>10 members) of historical and SSP simulations. The main difference between the CMIP5 and CMIP6 ensembles is that the historical simulations extend to 2005 for CMIP5 but to 2014 for CMIP6. Thus, for the period up until 2022, we use RCP8.5 scenario for CMIP5 models and SSP245 or SSP370 scenario for CMIP6 models (see Table S1). Because forcing scenarios share similar trajectories early on in the 21st century, we expect this to cause little variation across model ensembles (Lehner et al., 2020).

129

130

131

132

133

134

135

136

137

We compute the SO SST index as the spatial average of the SST over  $50^{\circ}\text{S} - 70^{\circ}\text{S}$  following DM2017. The DJF seasonal-mean SAM index is computed as the difference between zonal-mean SLP at  $45^{\circ}\text{S}$  and  $60^{\circ}\text{S}$ , normalized by the 1971–2000 average, following G. J. Marshall (2003). We focus on DJF SAM because the recent SAM trend is only significant in DJF (Swart & Fyfe, 2012; Waugh et al., 2020) and has been robustly attributed to stratospheric ozone depletion (Polvani et al., 2011; Banerjee et al., 2020). For both observations and GCM outputs, we remove the linear trend in DJF SAM and monthly SO SST timeseries over the entire period 1950–2022, before we perform the regression analysis.

138

## 2.2 Results

139

140

141

142

143

144

145

146

147

148

149

150

151

152

153

We begin with SO SST regressions against DJF SAM in observations, to examine whether DJF SAM anomalies are followed by anomalous SO SST. That is, we regress the timeseries of the DJF SAM index onto SO SST in every calendar month, ranging from the same year’s December to next year’s November. Fig. 2 clearly shows that positive DJF SAM anomalies lead to SO SST cooling, which peaks in the same season (DJF) and gradually weakens in the following two seasons before eventually vanishing at the end of the year. This independently confirms the findings of DM2017, who showed that the SAM impact on SO SST (derived from a shorter time period of 1981–2017 in that study) is highly seasonal and does not persist over a year. Furthermore, our analysis reveals that the annually-averaged SST anomaly following a unit of positive SAM is only  $-0.05\text{ K}$  (Fig. 2a) and the portion of SST variance explained ( $r^2$ ) is merely 0.2 (Fig. 2b). Therefore, while positive SAM can indeed lead to SO SST cooling, we emphasize that this modulation occurs only on a seasonal timescale and can barely sustain at interannual or longer timescales. A similar result was reported by Polvani et al. (2021) for the DJF SAM modulation of Antarctic SIE.

154

155

156

157

158

159

Next, we repeat this regression analysis with model large ensembles. Perhaps surprisingly, models well reproduce the observed relationship between the DJF SAM and monthly SO SST (Fig. 2a, b grey lines), despite failing to simulate multi-decadal SO cooling (Fig. 1c). In fact, the multi-model mean regression even overestimates the maximum DJF SO SST cooling response and accounts for a higher SO SST variance (higher  $r^2$ ) (also see Fig. S1 and S2 for individual models).

160

161

162

163

164

165

166

To further investigate how the SAM modulation of SO SST impacts model-simulated long-term SST trends, we separate all model ensemble members (365 in total) into two groups: one consisting of all the members that simulate a negative trend of SO SST over 1979–2022 (35 members, blue lines in Fig. 2) and the other consisting of the rest of members (330 members, orange lines in Fig. 2). Although the ensemble members that can simulate the long-term SO cooling all produce a stronger SST cooling response to SAM, the members that fail to simulate the long-term cooling are also able to capture or even

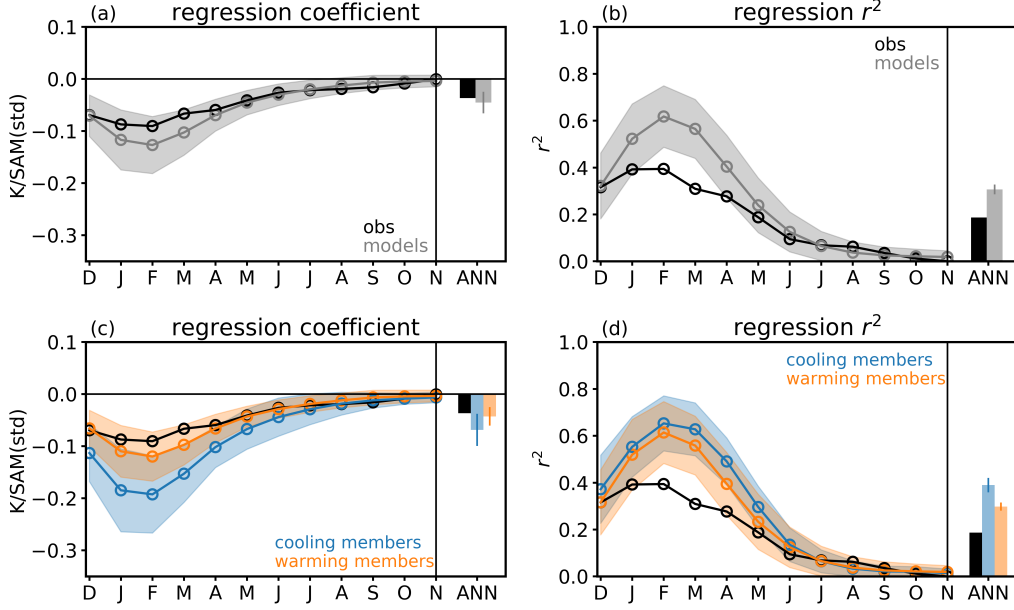


**Figure 2.** Regressions of monthly Southern Ocean SST (starting from DJF) onto same year’s DJF SAM. (a-c) regression coefficient; (b-d)  $r^2$  values of the regressions. Observations are shown in black, multi-model multi-ensemble means in grey, the ensemble members that simulate a negative SO SST trend over 1979–2022 (“cooling members”) in blue, and the members that simulate a positive SO SST trend (“warming members”) in orange. All shadings denote one standard deviation across ensemble members.

167 overestimate the observed SST response to SAM. These results suggest that correctly  
 168 simulating the seasonal-to-interannual SAM modulation of SO SST does not guarantee  
 169 the model’s performance on multi-decadal SO SST trends, implying that short-term and  
 170 long-term SST variability may be caused by different processes in models.

### 171 3 Low-frequency variability in the Southern Ocean

172 In the previous section, we have shown that in both observations and models the  
 173 SO SST cooling response to positive SAM anomalies only occurs in the same and fol-  
 174 lowing seasons. This raises a key question: Given the observed long-term SAM trend,  
 175 to what extent does the short-term SAM-SST relationship contribute to the observed  
 176 long-term SO cooling?

177 In the case of Antarctic SIE, Polvani et al. (2021) addressed this question by compar-  
 178 ing the actual SIE trend in observation with the estimate based on the SAM-SIE reg-  
 179 ression. They found that the long-term SAM-regressed SIE trend is much smaller than  
 180 the actual SIE trend, suggesting that the SAM is not the major driver of the observed  
 181 long-term SIE trend. We performed the same analysis for the SO SST and found a sim-  
 182 ilar result: the SAM-regressed annual-mean SO SST trend (1979–2022) is only 40% of  
 183 the actual SO SST trend. However, such an analysis using the zonal-mean SAM index  
 184 may overlook the spatial heterogeneity in the variability of winds and SST, and the re-  
 185 constructed SST trend may also be sensitive to the time period selected (an issue reported  
 186 by Polvani et al. 2021). Therefore, in this section, we revisit this question by employ-  
 187 ing a novel statistical method called low-frequency component analysis (LFCA; Wills et

188 al., 2018), to identify modes of low-frequency variability in observed zonal winds and the  
 189 SST changes associated with them.

### 190 3.1 LFCA method

191 LFCA (Wills et al., 2018) is a relatively new statistical technique – similar to the  
 192 conventional principal component analysis – to compute a linear combination of empir-  
 193 ical orthogonal functions (EOFs). LFCA maximizes the ratio of low-pass filtered vari-  
 194 ance to total variance, such that it isolates leading modes of low-frequency variability  
 195 and extracts physically-based modes in spatial-temporal signals in climate fields. It has  
 196 been applied to examine a wide range of climate quantities, including variability in global  
 197 SST anomalies (Wills et al., 2022), Atlantic ocean heat transport (Oldenburg et al., 2021),  
 198 and Arctic and Antarctic sea-ice concentration (Dörr et al., 2023; Bonan et al., 2023).

199 There are several advantages of using LFCA to investigate the relationship between  
 200 long-term SAM and SST. First, it helps separate low-frequency (decadal to multi-decadal)  
 201 and high-frequency (interannual) variability in SAM, allowing us to isolate the long-term  
 202 contribution of SAM to SST trends. Second, instead of directly using the simpler zonal-  
 203 mean SAM timeseries, we apply LFCA to the observed zonal winds at 850 hPa at each  
 204 latitude and longitude and find the timeseries associated with the leading mode of wind  
 205 variability. This gives us a more complete understanding of the relationship between winds  
 206 and SST as it accounts for spatial variability of winds and SST. This is important be-  
 207 cause several recent studies have pointed out the non-zonal feature of the observed SAM-  
 208 associated wind changes (Vaugh et al., 2020) and its zonally asymmetric impacts on SO  
 209 and remote SSTs (Dong, Armour, et al., 2022).

210 Our analysis uses the observed zonal winds at 850 hPa (U850) from the ERA5 Re-  
 211 analysis dataset (Hersbach et al., 2020). As with the SAM index analyzed in section 2,  
 212 we consider DJF U850 over 1950–2022. We apply LFCA to the observed U850 only over  
 213 40°S – 80°S, to avoid variability associated with tropical winds. Our LFCA uses a 15-  
 214 year cutoff low-pass filter to isolate low-frequency variability, and we retain the 5 lead-  
 215 ing EOFs, which account for 77% of the total U850 variability (we find that increasing  
 216 the number of EOFs does not lead to substantially more variance explained). The LFCA  
 217 results remain the same regardless we choose a low-pass filter of 10 year, 15 year or 20  
 218 year (compare Fig. S3 to Fig. 3).

### 219 3.2 LFCA results

220 First, let us consider the leading anomaly patterns (i.e., low-frequency patterns,  
 221 LFPs) and their associated timeseries (i.e., low-frequency components, LFCs) obtained  
 222 by applying LFCA to the observed DJF U850 over the Southern Ocean. The first 5 LFPs  
 223 and LFCs are shown in Fig. 3, in the left and right columns, respectively.

224 The leading mode (LFP1) features a SAM-like annular pattern of wind strength-  
 225 ening that has increased monotonically from 1970s to 2000s (see LFC1). This is well in  
 226 line with the SAM trend caused by ozone depletion (Banerjee et al., 2020). This mode  
 227 accounts for 58.3% of the low-frequency variance and has the highest signal-to-noise ra-  
 228 tio of 0.4. The next four modes exhibit mostly non-zonal patterns (LFP2-5), where wind  
 229 anomalies are confined to specific ocean sectors. The LFCs associated with LFP2 and  
 230 LFP3 have some decadal-to-multi-decadal variability, while the LFCs associated with  
 231 LFP4 and LFP5 are dominated by interannual variability, consistent with their low signal-  
 232 to-noise ratio.

233 Next, we examine the U850 trend pattern (1979–2022) associated with each mode  
 234 by projecting each LFC onto the corresponding LFP of U850 at each grid point over the  
 235 SO. Fig. S4 confirms that the total reconstruction based on the five LFPs (Fig. S4b) well  
 236 reproduces the observed U850 trend pattern (Fig. S4a), which is characterized by a strength-

237 ening of the westerlies at high latitudes in the Southern Ocean. Furthermore, the total  
 238 reconstructed trend pattern remains the same using either the leading five or three LFPs,  
 239 suggesting that LFP 1-3 are the major contributor to the total U850 trends over recent  
 240 decades.

### 241 3.3 Long-term relationship between SO SST and winds

242 Having established that the leading modes obtained by LFCA well reproduce the  
 243 observed U850 trend pattern, we next investigate the long-term relationship between U850  
 244 and SO SST by examining how each LFP and LFC influences SST across timescales.

245 First, we regress the observed DJF SST over the entire period (1950–2022) at each  
 246 grid box onto the LFC timeseries associated with the three leading wind LFPs, respec-  
 247 tively (Fig. 4 a-c). We focus on DJF SST as our earlier results suggest it is the season  
 248 when the SAM, through surface winds, has the strongest impact on SST. Consistent with  
 249 the SAM-SST regression result (Fig. 2), the wind LFC-SST regression also shows broad  
 250 SST cooling anomalies around Antarctica associated with positive LFC anomalies. How-  
 251 ever, it is interesting that the patterns of SST cooling response do not quite match the  
 252 wind anomaly patterns (compare Fig. 3 and Fig. 4): All three wind LFPs feature posi-  
 253 tive wind anomalies throughout the Southern Ocean (LFP1 even has stronger wind anoma-  
 254 lies in the Atlantic basin than in the Pacific basin), yet their SST cooling responses are  
 255 most significant in the Pacific basin. This mismatch in spatial patterns may give us a  
 256 first hint that the proposed mechanism linking surface winds to SO SST through Ekman  
 257 heat transport may not sufficiently explain the spatial patterns of wind-SST relation-  
 258 ship.

259 Second, we estimate the long-term SST trends over the period 1979–2022 based on  
 260 the above linear regression. Specifically, we multiply the regression between each LFC  
 261 and SST at each grid box with the corresponding LFC, and then take the linear trend  
 262 of the reconstructed SST timeseries at each grid box (Fig. 4). Although the LFC-based  
 263 SST trends also occur in the Pacific basin – consistent with observations – one imme-  
 264 diately sees that the magnitudes of wind-driven SST trends are much weaker than that  
 265 observed (cf. Fig. 4 middle row vs. Fig. 4g). Taking a spatial average over the Pacific  
 266 sector of the Southern Ocean where the observed SST cooling is strongest (150°E – 60°W,  
 267 50°S – 70°S), we obtain an SST trend of  $-0.98$  °C/decade from the observation, and SST  
 268 trends of  $-0.25$ ,  $-0.14$  and  $-0.02$  °C/decade from LFC1-3 regressions respectively, which  
 269 altogether account for less than half of the actual SST trend (Fig. 4i). To further illus-  
 270 trate the inability of winds to account for the time-evolution of SO SST, we plot the time-  
 271 series of DJF SO SST anomalies (relative to their climatology) for the observation and  
 272 for the estimates using LFC1-3 regressions (Fig. 4h). Although each of the LFCs con-  
 273 tributes to some SST variability, none of them can produce a multi-decadal SO SST vari-  
 274 ability as strong as the observed timeseries. Even the sum of all three LFC-regression-  
 275 based SO SST timeseries fails to explain the much larger multi-decadal trends in the ob-  
 276 served SO SST.

277 Furthermore, our SST trend estimates so far have been focused on DJF, in the same  
 278 season with wind anomalies, so as to capture the strongest wind impacts on SST. We  
 279 also repeated the analysis for annual-mean (instead of DJF only) SST (Fig. S5). The  
 280 annual-mean SST anomalies following a unit of DJF wind LFC changes are even weaker,  
 281 leading to almost negligible wind-driven annual-mean SST trends over recent decades,  
 282 i.e.,  $-0.16$  °C/decade over 1979–2022 from all three leading-mode regressions, compared  
 283 to  $-0.9$  °C/decade of the actual SST trend (Fig. S5j).

284 Thus, by projecting SO SST onto the leading modes of observed wind variability,  
 285 we find that although positive DJF wind anomalies can cause some SST cooling in the  
 286 same season, this modulation does not survive more than a few months, and the result-  
 287 ing wind-driven SST cooling is *too weak* to explain the large multi-decadal trend in the

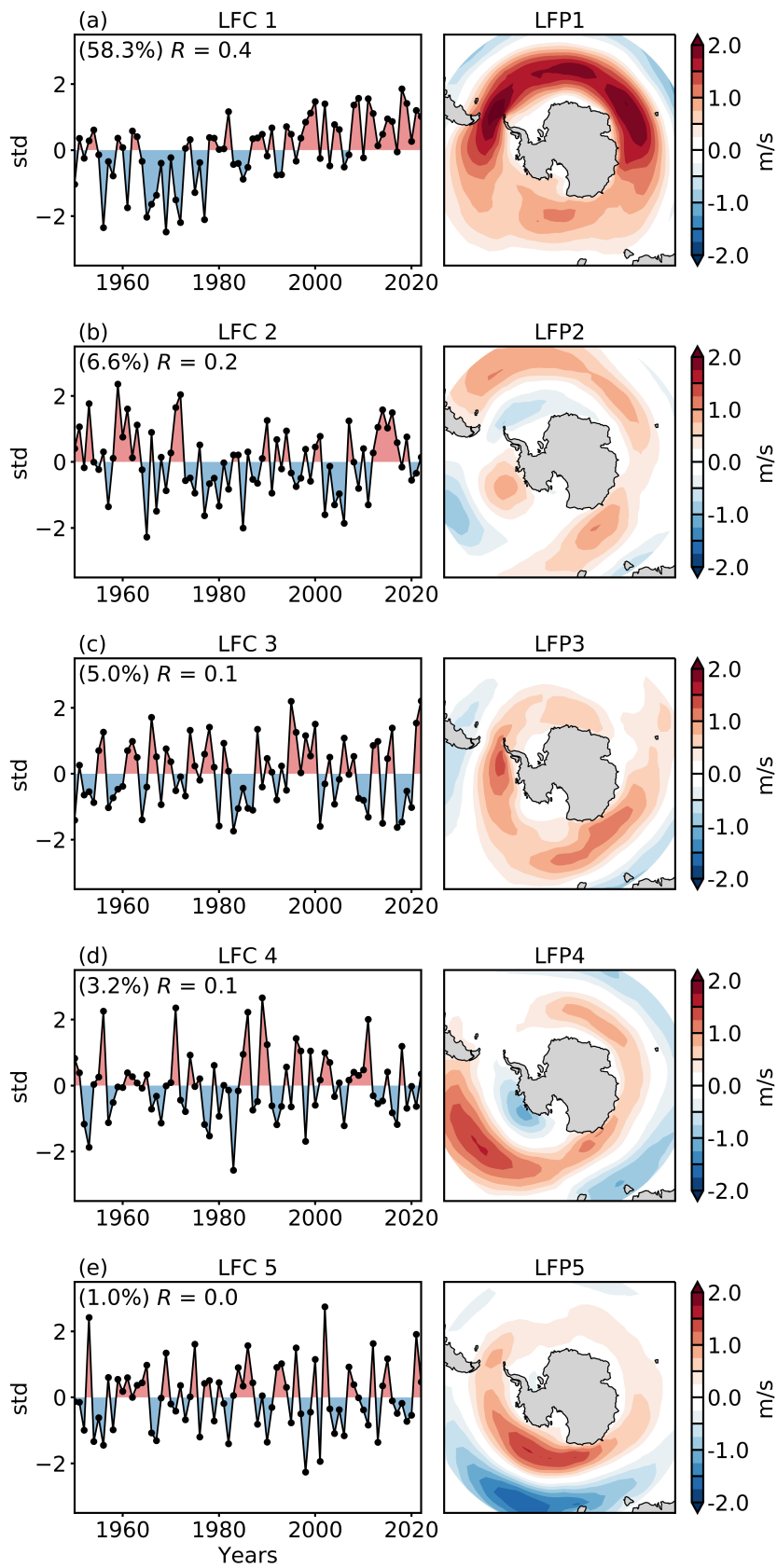


**Figure 3.** Low-frequency patterns (LFP; right column; unit: m/s) and their associated components (LFC; left column; unit: standard deviation) for the observed DJF U850 wind anomalies. Values in parentheses in the LFC panels denote the low-frequency variance explained by each mode.  $R$  values denote the ratio of low-frequency variance explained to the total variance, representing the signal-to-noise ratio.

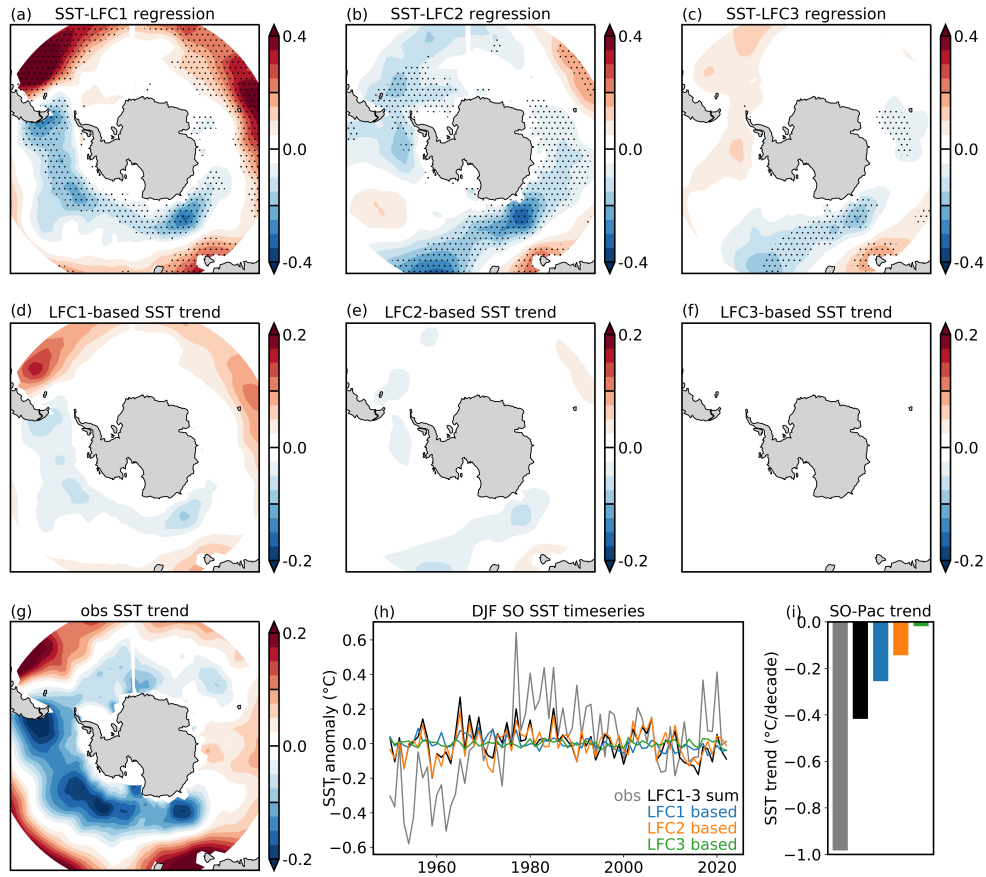


**Figure 4.** (a-c) DJF SST regression map onto LFC1-3 respectively (unit:  $^{\circ}\text{C}/\text{std}$ ). Stippling indicates where linear regression is statistically significant at 95% level. (d-g) DJF SST trend patterns over 1979–2022 ( $^{\circ}\text{C}/\text{decade}$ ) estimated from regressions with LFC 1-3 respectively and ERSSTv5. (i) Timeseries of SO SST anomalies relative to their climatology and (j) SST trends averaged over the Pacific sector over 1979–2022, from the observation (grey), the regressions with LFC1-3 respectively (colored), and all three leading LFCs (black).

288 observed Southern Ocean SST (Fig. 4). Hence, the recent wind strengthening over the  
 289 Southern Ocean is unlikely the key driver of the long-term Southern Ocean cooling.

## 290 4 Summary and Discussion

291 In this study, we have re-examined a previously proposed idea that positive SAM  
 292 anomalies in DJF, associated with a strengthening of the circumpolar westerlies, may  
 293 in part explain the observed Southern Ocean cooling (J. Marshall et al., 2014; Ferreira  
 294 et al., 2015; Doddridge & Marshall, 2017; Kostov et al., 2018; Hartmann, 2022). Using  
 295 GCM large-ensembles, we have found that models are able to capture the observed seasonal-  
 296 to-interannual modulation of SO SST by the SAM, regardless of whether they are able

297 to simulate the long-term SO cooling. Focusing on observations, we have shown that al-  
298 though positive SAM anomalies and positive zonal wind anomalies in DJF can lead to  
299 some SST cooling anomalies in the same season, this mechanism only operates for a few  
300 months and does not persist from year to year. These results suggest that the SAM mod-  
301 ulation of SO SST, via the strengthening of SO westerlies, is too weak to explain the ob-  
302 served multi-decadal Southern Ocean cooling.

303 One novel aspect of our study is that we used a low-frequency component analy-  
304 sis to isolate trends in SO zonal winds, rather than focusing on trends in the SAM. While  
305 the SAM index has been widely used as a metric to quantify zonal wind changes in the  
306 Southern Hemisphere, it only represents zonal-mean features and includes a wide range  
307 of variabilities from interannual to decadal timescales. Applying LFCA to the observed  
308 wind anomalies has allowed us to (1) obtain the timeseries (LFCs) of the leading modes  
309 of wind variability while retaining the spatial pattern of the wind anomalies, and (2) dis-  
310 entangle low-frequency from high-frequency variability.

311 It could be argued that the weak connection between long-term SAM and SST trends  
312 can be immediately deduced from the SAM and SST timeseries alone. A simple visual  
313 inspection of their smoothed timeseries (thick curves in Fig. 1a and b, respectively) suf-  
314 fices to note that the kinks in those curves do not match. The SST cooling starts after  
315 1980 and persists past 2010, whereas the positive SAM trend starts well before 1970 and  
316 stops after 2000, as a consequence of the Montreal Protocol (Banerjee et al., 2020). Build-  
317 ing on this, our new analysis, accounting for spatial-temporal variability, adds additional  
318 evidence corroborating the inability of the SAM and surface westerlies to explain the re-  
319 cent multi-decadal SO cooling.

320 Understanding the causes of the observed Southern Ocean cooling and biases in  
321 climate models remains a major challenge. By showing that the SAM-driven SST cool-  
322 ing is too weak to explain the long-term SO SST trends, our results point to a possibly  
323 limited role of stratospheric ozone depletion. This finding is also consistent with recent  
324 modeling evidence that nudging tropospheric wind anomalies around Antarctica towards  
325 observations in a GCM (CESM1) does not produce significant SO SST cooling over re-  
326 cent four decades (Blanchard-Wrigglesworth et al., 2021; Dong, Armour, et al., 2022).  
327 Thus, the impact of the Antarctic ozone hole on long-term SO SST via the SAM appears  
328 to be less robust than previously proposed. Even so, there is evidence that the ozone hole  
329 has caused remote climate impacts on lower latitudes, notably on subtropical precipi-  
330 tation (Kang et al., 2011; Gonzalez et al., 2014; Wu & Polvani, 2017). The Antarctic ozone  
331 hole, therefore, may have impacted SST in remote regions (e.g., the tropical Pacific), and  
332 those impacts could then have been communicated back to the Southern Ocean SST via  
333 atmospheric teleconnections (Ding et al., 2011; Meehl et al., 2016; Chung et al., 2022;  
334 Dong, Armour, et al., 2022). Such complex two-way teleconnections, however, remain  
335 largely unexplored.

336 Beyond potential remote impacts from the tropics, other local contributors to the  
337 recent SO cooling remain plausible, including freshwater input from Antarctic ice-sheet  
338 melt or more equatorward sea-ice melt (Purich et al., 2018; Bintanja et al., 2013; Rye  
339 et al., 2020; Dong, Pauling, et al., 2022; Haumann et al., 2020), and Southern Ocean nat-  
340 ural variability (Latif et al., 2013; Cabré et al., 2017; Zhang et al., 2019). Whether the  
341 recent SO cooling was driven by historical forcings or simply reflects natural variabil-  
342 ity has important implications for SST trends in the near future. Accurately constrain-  
343 ing future projections of Antarctic climate change thus requires a better understanding  
344 of the causes of the recent multi-decadal Southern Ocean SST trends.

## 345 **Acknowledgments**

346 YD was supported by the NOAA Climate and Global Change Postdoctoral Fellowship  
347 Program, administered by UCAR's Cooperative Programs for the Advancement of Earth

348 System Science (CPAESS) under award NA210AR4310383. DBB was supported by the  
 349 National Science Foundation (NSF) Graduate Research Fellowship Program (NSF Grant  
 350 DGE-1745301). LMP is grateful to the US NSF for their continued support, under award  
 351 #1914569.

## 352 Data Availability Statement

353 ERSSTv5 SST data is available at <https://psl.noaa.gov/data/gridded/data.noaa.ersst.v5.html>.  
 354 ERA5 reanalysis SLP and U850 data is available from the Copernicus Climate Service  
 355 at <https://cds.climate.copernicus.eu/>. CMIP5 and CMIP6 model multi-model large en-  
 356 sembles are available via the NCAR Climate Data Gateway and via the ESGF archive  
 357 at: <https://esgf-node.llnl.gov/search/cmip6/>.

## 358 References

- 359 Armour, K. C., Marshall, J., Scott, J. R., Donohoe, A., & Newsom, E. R. (2016).  
 360 Southern Ocean warming delayed by circumpolar upwelling and equatorward  
 361 transport. *Nature Geoscience*, *9*(7), 549–554.
- 362 Banerjee, A., Fyfe, J. C., Polvani, L. M., Waugh, D., & Chang, K.-L. (2020). A  
 363 pause in Southern Hemisphere circulation trends due to the Montreal Protocol.  
 364 *Nature*, *579*(7800), 544–548.
- 365 Bintanja, R., van Oldenborgh, G. J., Drijfhout, S., Wouters, B., & Katsman, C.  
 366 (2013). Important role for ocean warming and increased ice-shelf melt in  
 367 Antarctic sea-ice expansion. *Nature Geoscience*, *6*(5), 376–379.
- 368 Bitz, C., & Polvani, L. M. (2012). Antarctic climate response to stratospheric ozone  
 369 depletion in a fine resolution ocean climate model. *Geophysical Research Let-  
 370 ters*, *39*(20).
- 371 Blanchard-Wrigglesworth, E., Roach, L. A., Donohoe, A., & Ding, Q. (2021). Impact  
 372 of winds and Southern Ocean SSTs on Antarctic sea ice trends and variability.  
 373 *Journal of Climate*, *34*(3), 949–965.
- 374 Bonan, D. B., Dörr, J., Wills, R. C., Thompson, A. F., & Årthun, M. (2023).  
 375 Sources of low-frequency variability in observed Antarctic sea ice. *EGU sphere*,  
 376 *2023*, 1–28.
- 377 Cabré, A., Marinov, I., & Gnanadesikan, A. (2017). Global atmospheric tele-  
 378 connections and multidecadal climate oscillations driven by Southern Ocean  
 379 convection. *Journal of Climate*, *30*(20), 8107–8126.
- 380 Chung, E.-S., Kim, S.-J., Timmermann, A., Ha, K.-J., Lee, S.-K., Stuecker, M. F., et  
 381 al. (2022). Antarctic sea-ice expansion and Southern Ocean cooling linked to  
 382 tropical variability. *Nature Climate Change*, *12*(5), 461–468.
- 383 De Lavergne, C., Palter, J. B., Galbraith, E. D., Bernardello, R., & Marinov, I.  
 384 (2014). Cessation of deep convection in the open Southern Ocean under an-  
 385 thropogenic climate change. *Nature Climate Change*, *4*(4), 278–282.
- 386 Deser, C., Lehner, F., Rodgers, K. B., Ault, T., Delworth, T. L., DiNezio, P. N.,  
 387 ... others (2020). Insights from Earth system model initial-condition large  
 388 ensembles and future prospects. *Nature Climate Change*, *10*(4), 277–286.
- 389 Ding, Q., Steig, E. J., Battisti, D. S., & Küttel, M. (2011). Winter warming in West  
 390 Antarctica caused by central tropical Pacific warming. *Nature Geoscience*,  
 391 *4*(6), 398–403.
- 392 Doddridge, E. W., & Marshall, J. (2017). Modulation of the seasonal cycle of  
 393 Antarctic sea ice extent related to the Southern Annular Mode. *Geophysical  
 394 Research Letters*, *44*(19), 9761–9768.
- 395 Dong, Y., Armour, K. C., Battisti, D. S., & Blanchard-Wrigglesworth, E. (2022).  
 396 Two-way teleconnections between the Southern Ocean and the tropical Pacific  
 397 via a dynamic feedback. *Journal of Climate*, 1–37.

- 398 Dong, Y., Pauling, A. G., Sadai, S., & Armour, K. C. (2022). Antarctic ice-sheet  
399 meltwater reduces transient warming and climate sensitivity through the sea-  
400 surface temperature pattern effect. *Geophysical Research Letters*, *49*(24),  
401 e2022GL101249.
- 402 Dörr, J. S., Bonan, D. B., Árrthun, M., Svendsen, L., & Wills, R. C. (2023). Forced  
403 and internal components of observed Arctic sea-ice changes. *The Cryosphere*  
404 *Discussions*, 1–27.
- 405 Fan, T., Deser, C., & Schneider, D. P. (2014). Recent Antarctic sea ice trends in  
406 the context of Southern Ocean surface climate variations since 1950. *Geophys-  
407 ical Research Letters*, *41*(7), 2419–2426.
- 408 Ferreira, D., Marshall, J., Bitz, C. M., Solomon, S., & Plumb, A. (2015). Antarc-  
409 tic Ocean and sea ice response to ozone depletion: A two-time-scale problem.  
410 *Journal of Climate*, *28*(3), 1206–1226.
- 411 Gonzalez, P. L., Polvani, L. M., Seager, R., & Correa, G. J. (2014). Stratospheric  
412 ozone depletion: a key driver of recent precipitation trends in South Eastern  
413 South America. *Climate Dynamics*, *42*, 1775–1792.
- 414 Gupta, A. S., & England, M. H. (2006). Coupled ocean–atmosphere–ice response  
415 to variations in the southern annular mode. *Journal of Climate*, *19*(18), 4457–  
416 4486.
- 417 Hall, A., & Visbeck, M. (2002). Synchronous variability in the Southern Hemi-  
418 sphere atmosphere, sea ice, and ocean resulting from the annular mode. *Jour-  
419 nal of Climate*, *15*(21), 3043–3057.
- 420 Hartmann, D. L. (2022). The Antarctic ozone hole and the pattern effect on cli-  
421 mate sensitivity. *Proceedings of the National Academy of Sciences*, *119*(35),  
422 e2207889119.
- 423 Haumann, F. A., Gruber, N., & Münnich, M. (2020). Sea-ice induced southern  
424 ocean subsurface warming and surface cooling in a warming climate. *AGU Ad-  
425 vances*, *1*(2), e2019AV000132.
- 426 Hersbach, H., Bell, B., Berrisford, P., Hirahara, S., Horányi, A., Muñoz-Sabater, J.,  
427 ... others (2020). The ERA5 global reanalysis. *Quarterly Journal of the Royal*  
428 *Meteorological Society*, *146*(730), 1999–2049.
- 429 Huang, B., Thorne, P. W., Banzon, V. F., Boyer, T., Chepurin, G., Lawrimore,  
430 J. H., ... Zhang, H.-M. (2017). Extended reconstructed sea surface tem-  
431 perature, version 5 (ERSSTv5): upgrades, validations, and intercomparisons.  
432 *Journal of Climate*, *30*(20), 8179–8205.
- 433 Hwang, Y.-T., Xie, S.-P., Deser, C., & Kang, S. M. (2017). Connecting tropical cli-  
434 mate change with southern ocean heat uptake. *Geophysical Research Letters*,  
435 *44*(18), 9449–9457.
- 436 Kang, S. M., Polvani, L. M., Fyfe, J., & Sigmond, M. (2011). Impact of polar ozone  
437 depletion on subtropical precipitation. *Science*, *332*(6032), 951–954.
- 438 Kang, S. M., Xie, S.-P., Shin, Y., Kim, H., Hwang, Y.-T., Stuecker, M. F., et al.  
439 (2020). Walker circulation response to extratropical radiative forcing. *Science*  
440 *advances*, *6*(47), eabd3021.
- 441 Kang, S. M., Yu, Y., Deser, C., Zhang, X., Kang, I.-S., Lee, S.-S., ... Ceppi, P.  
442 (2023). Global impacts of recent Southern Ocean cooling. *Proceedings of the*  
443 *National Academy of Sciences*, *120*(30), e2300881120.
- 444 Kim, H., Kang, S. M., Kay, J. E., & Xie, S.-P. (2022). Subtropical clouds key to  
445 Southern Ocean teleconnections to the tropical pacific. *Proceedings of the Na-  
446 tional Academy of Sciences*, *119*(34), e2200514119.
- 447 Kostov, Y., Ferreira, D., Armour, K. C., & Marshall, J. (2018). Contributions of  
448 greenhouse gas forcing and the Southern Annular Mode to historical South-  
449 ern Ocean surface temperature trends. *Geophysical Research Letters*, *45*(2),  
450 1086–1097.
- 451 Landrum, L. L., Holland, M. M., Raphael, M. N., & Polvani, L. M. (2017). Strato-  
452 spheric ozone depletion: An unlikely driver of the regional trends in antarctic

- 453 sea ice in austral fall in the late twentieth century. *Geophysical Research*  
 454 *Letters*, *44*(21), 11–062.
- 455 Latif, M., Martin, T., & Park, W. (2013). Southern Ocean sector centennial climate  
 456 variability and recent decadal trends. *Journal of Climate*, *26*(19), 7767–7782.
- 457 Lefebvre, W., Goosse, H., Timmermann, R., & Fichefet, T. (2004). Influence of the  
 458 Southern Annular Mode on the sea ice–ocean system. *Journal of Geophysical*  
 459 *Research: Oceans*, *109*(C9).
- 460 Lehner, F., Deser, C., Maher, N., Marotzke, J., Fischer, E. M., Brunner, L., ...  
 461 Hawkins, E. (2020). Partitioning climate projection uncertainty with multiple  
 462 large ensembles and CMIP5/6. *Earth System Dynamics*, *11*(2), 491–508.
- 463 Marshall, G. J. (2003). Trends in the Southern Annular Mode from observations and  
 464 reanalyses. *Journal of climate*, *16*(24), 4134–4143.
- 465 Marshall, J., Armour, K. C., Scott, J. R., Kostov, Y., Hausmann, U., Ferreira, D.,  
 466 ... Bitz, C. M. (2014). The ocean’s role in polar climate change: asymmetric  
 467 Arctic and Antarctic responses to greenhouse gas and ozone forcing. *Philo-*  
 468 *sophical Transactions of the Royal Society A: Mathematical, Physical and*  
 469 *Engineering Sciences*, *372*(2019), 20130040.
- 470 Meehl, G. A., Arblaster, J. M., Bitz, C. M., Chung, C. T., & Teng, H. (2016).  
 471 Antarctic sea-ice expansion between 2000 and 2014 driven by tropical Pacific  
 472 decadal climate variability. *Nature Geoscience*, *9*(8), 590–595.
- 473 Oldenburg, D., Wills, R. C., Armour, K. C., Thompson, L., & Jackson, L. C. (2021).  
 474 Mechanisms of low-frequency variability in North Atlantic Ocean heat trans-  
 475 port and AMOC. *Journal of Climate*, *34*(12), 4733–4755.
- 476 Parkinson, C. L. (2019). A 40-y record reveals gradual Antarctic sea ice increases  
 477 followed by decreases at rates far exceeding the rates seen in the Arctic. *Pro-*  
 478 *ceedings of the National Academy of Sciences*, *116*(29), 14414–14423.
- 479 Pauling, A. G., Bitz, C. M., Smith, I. J., & Langhorne, P. J. (2016). The response  
 480 of the Southern Ocean and Antarctic sea ice to freshwater from ice shelves in  
 481 an Earth system model. *Journal of Climate*, *29*(5), 1655–1672.
- 482 Polvani, L. M., Banerjee, A., Chemke, R., Doddridge, E., Ferreira, D., Gnanade-  
 483 sikan, A., ... others (2021). Interannual sam modulation of antarctic sea ice  
 484 extent does not account for its long-term trends, pointing to a limited role for  
 485 ozone depletion. *Geophysical Research Letters*, *48*(21), e2021GL094871.
- 486 Polvani, L. M., & Smith, K. L. (2013). Can natural variability explain observed  
 487 Antarctic sea ice trends? New modeling evidence from CMIP5. *Geophysical*  
 488 *Research Letters*, *40*(12), 3195–3199.
- 489 Polvani, L. M., Waugh, D. W., Correa, G. J., & Son, S.-W. (2011). Stratospheric  
 490 ozone depletion: The main driver of twentieth-century atmospheric circulation  
 491 changes in the Southern Hemisphere. *Journal of Climate*, *24*(3), 795–812.
- 492 Previdi, M., & Polvani, L. M. (2014). Climate system response to stratospheric  
 493 ozone depletion and recovery. *Quarterly Journal of the Royal Meteorological*  
 494 *Society*, *140*(685), 2401–2419.
- 495 Purich, A., & England, M. H. (2023). Projected impacts of Antarctic meltwater  
 496 anomalies over the twenty-first century. *Journal of Climate*, *36*(8), 2703–2719.
- 497 Purich, A., England, M. H., Cai, W., Sullivan, A., & Durack, P. J. (2018). Impacts  
 498 of broad-scale surface freshening of the Southern Ocean in a coupled climate  
 499 model. *Journal of Climate*, *31*(7), 2613–2632.
- 500 Roach, L. A., Dörr, J., Holmes, C. R., Massonnet, F., Blockley, E. W., Notz, D., ...  
 501 others (2020). Antarctic sea ice area in CMIP6. *Geophysical Research Letters*,  
 502 *47*(9), e2019GL086729.
- 503 Rye, C. D., Marshall, J., Kelley, M., Russell, G., Nazarenko, L. S., Kostov, Y., ...  
 504 Hansen, J. (2020). Antarctic glacial melt as a driver of recent Southern Ocean  
 505 climate trends. *Geophysical Research Letters*, *47*(11), e2019GL086892.
- 506 Seviour, W. J. M., Codron, F., Doddridge, E. W., Ferreira, D., Gnanadesikan, A.,  
 507 Kelley, M., ... others (2019). The southern ocean sea surface temperature

- 508 response to ozone depletion: A multimodel comparison. *Journal of Climate*,  
509 *32*(16), 5107–5121.
- 510 Seviour, W. J. M., Gnanadesikan, A., & Waugh, D. W. (2016). The transient re-  
511 sponse of the Southern Ocean to stratospheric ozone depletion. *Journal of Cli-*  
512 *mate*, *29*(20), 7383–7396.
- 513 Sigmond, M., & Fyfe, J. C. (2014). The Antarctic sea ice response to the ozone hole  
514 in climate models. *Journal of Climate*, *27*(3), 1336–1342.
- 515 Smith, K. L., Polvani, L. M., & Marsh, D. R. (2012). Mitigation of 21st century  
516 Antarctic sea ice loss by stratospheric ozone recovery. *Geophysical Research*  
517 *Letters*, *39*(20).
- 518 Swart, N., & Fyfe, J. C. (2012). Observed and simulated changes in the South-  
519 ern Hemisphere surface westerly wind-stress. *Geophysical Research Letters*,  
520 *39*(16).
- 521 Thompson, D. W., & Solomon, S. (2002). Interpretation of recent Southern Hemi-  
522 sphere climate change. *Science*, *296*(5569), 895–899.
- 523 Waugh, D. W., Banerjee, A., Fyfe, J. C., & Polvani, L. M. (2020). Contrasting  
524 recent trends in Southern Hemisphere Westerlies across different ocean basins.  
525 *Geophysical Research Letters*, *47*(18), e2020GL088890.
- 526 Wills, R. C., Dong, Y., Proistosescu, C., Armour, K. C., & Battisti, D. S. (2022).  
527 Systematic climate model biases in the large-scale patterns of recent sea-  
528 surface temperature and sea-level pressure change. *Geophysical Research*  
529 *Letters*, *49*(17), e2022GL100011.
- 530 Wills, R. C., Schneider, T., Wallace, J. M., Battisti, D. S., & Hartmann, D. L.  
531 (2018). Disentangling global warming, multidecadal variability, and el niño in  
532 Pacific temperatures. *Geophysical Research Letters*, *45*(5), 2487–2496.
- 533 Wu, Y., & Polvani, L. M. (2017). Recent trends in extreme precipitation and tem-  
534 perature over southeastern South America: The dominant role of stratospheric  
535 ozone depletion in the CESM Large Ensemble. *Journal of Climate*, *30*(16),  
536 6433–6441.
- 537 Zhang, L., Delworth, T. L., Cooke, W., & Yang, X. (2019). Natural variability of  
538 Southern Ocean convection as a driver of observed climate trends. *Nature Cli-*  
539 *mate Change*, *9*(1), 59–65.

1 **Recent multi-decadal Southern Ocean surface cooling**  
2 **unlikely caused by Southern Annular Mode trends**

3 **Yue Dong<sup>1,2</sup>, Lorenzo M. Polvani<sup>1,3</sup>, David B. Bonan<sup>4</sup>**

4 <sup>1</sup>Lamont-Doherty Earth Observatory, Columbia University, Palisades, NY, USA

5 <sup>2</sup>Cooperative Programs for the Advancement of Earth System Science, University Corporation for

6 Atmospheric Research, Boulder, CO, USA

7 <sup>3</sup>Department of Applied Physics and Applied Mathematics, Columbia University, New York, NY, USA

8 <sup>4</sup>Environmental Science and Engineering, California Institute of Technology, Pasadena, CA, USA

9 **Key Points:**

- 10 • Austral summer SAM variability affects Southern Ocean SST only on seasonal to  
11 interannual timescales
- 12 • The short-term SAM-SST relationship makes little contribution to the observed  
13 multi-decadal Southern Ocean SST trends
- 14 • GCMs capture the observed seasonal SAM-SST relationship and yet fail to sim-  
15 ulate the observed long-term SO cooling

---

Corresponding author: Yue Dong, [dongyueatmos@gmail.com](mailto:dongyueatmos@gmail.com)

## Abstract

Over recent decades, the Southern Ocean (SO) has experienced multi-decadal surface cooling despite global warming. Earlier studies have proposed that recent SO cooling has been caused by the strengthening of surface westerlies associated with a positive trend of the Southern Annular Mode (SAM) forced by ozone depletion. Here we revisit this hypothesis by examining the relationships between the SAM, zonal winds and SO sea-surface temperature (SST). Using a low-frequency component analysis, we show that while positive SAM anomalies can induce SST cooling as previously found, this seasonal-to-interannual modulation makes only a small contribution to the observed long-term SO cooling. Global climate models well capture the observed interannual SAM-SST relationship, and yet generally fail to simulate the observed multi-decadal SO cooling. The forced SAM trend in recent decades is thus unlikely the main cause of the observed SO cooling, pointing to a limited role of the Antarctic ozone hole.

## Plain Language Summary

Under increased greenhouse gases, the Southern Ocean sea-surface temperatures have cooled over the recent several decades. The cause of Southern Ocean cooling remains a puzzling feature of recent climate change. Earlier studies have proposed that this multi-decadal cooling in the Southern Ocean has arisen in part from the strengthening of surface winds associated with a positive trend in a mode of climate variability known as the Southern Annular Mode (SAM). Here we employ a new statistical method to examine this proposed relationship in both observations and climate models. We found that SAM variability only changes Southern Ocean surface temperature on short-term timescales and makes little contribution to observed long-term trends. Our results thus suggest the SAM trend, via the strengthening of circumpolar westerlies, is unlikely the main cause of the observed long-term Southern Ocean cooling.

## 1 Introduction

Unlike the Arctic, the Southern Ocean has experienced substantial cooling in recent decades, following an earlier warming period from the 1950s to 1980s (Fig. 1a). This multi-decadal surface cooling over the Southern Ocean has been accompanied by anomalous surface freshening, sub-surface warming, and an expansion of sea ice around Antarctica (Fan et al., 2014; De Lavergne et al., 2014; Armour et al., 2016; Parkinson, 2019; Roach et al., 2020), all of which remain puzzling features of the observed climate change in the Southern Hemisphere. Apart from its local impacts, Southern Ocean surface cooling has been found to have remote effects on the pattern of tropical surface warming (Hwang et al., 2017; Dong, Armour, et al., 2022; Kim et al., 2022), tropical atmospheric circulation (Kang et al., 2020, 2023), and estimates of the global warming rate and climate sensitivity (Dong, Pauling, et al., 2022).

Despite its broad impacts on both the local and global climate, the observed Southern Ocean SST trend remains poorly simulated by global climate models (GCMs) (Fig. 1c). GCM initial-condition large ensembles (Deser et al., 2020) generally produce too strong SO surface warming over recent decades (Wills et al., 2022), along with too weak surface freshening and positive trends in Antarctic sea-ice extent (Roach et al., 2020). These model deficiencies over the historical period thus call into question the reliability of model projections of future Antarctic climate change.

Several hypotheses have been put forward to explain the observed multi-decadal SO cooling, including SO natural variability driven by ocean convection (Polvani & Smith, 2013; Latif et al., 2013; Cabré et al., 2017; Zhang et al., 2019), freshwater input from Antarctic ice-sheet melt (Rye et al., 2020; Pauling et al., 2016; Bintanja et al., 2013; Purich et al., 2018; Purich & England, 2023) or from increased equatorward sea-ice melt (Haumann

et al., 2020). These hypotheses, however, are mostly built on modeling evidence, and are thus potentially subject to model biases. An alternative hypothesis is that the observed SO cooling trends may be driven by trends in surface westerlies via the Southern Annular Mode (SAM) through northward Ekman transport (Hall & Visbeck, 2002; Lefebvre et al., 2004; Gupta & England, 2006; Ferreira et al., 2015). It has been robustly observed that the surface westerlies have strengthened and shifted poleward, associated with the positive trend in the austral-summer (DJF) SAM over the second half of the 20th century (Thompson & Solomon, 2002; G. J. Marshall, 2003) (also Fig. 1b). This trend in SAM has been in large part attributed to stratospheric ozone depletion (Polvani et al., 2011; Previdi & Polvani, 2014; Banerjee et al., 2020). The observed SAM trend is generally well captured in GCM simulations (Fig. 1d) (Waugh et al., 2020).

To link SST variability to SAM variability, Doddridge and Marshall (2017) carried out an observational study and reported a robust interannual relationship between the SAM and SO SST. Their results show that positive SAM anomalies in the austral summer lead to anomalous cold SST persisting to the following autumn, suggesting a possible contribution of ozone depletion to SO cooling. On the modeling side, the SAM-SST connection on multi-decadal time scales was supported by idealized model simulations with abrupt SAM or ozone forcing (e.g., Ferreira et al., 2015; Kostov et al., 2018; Seviour et al., 2016). Early “step-like” forcing experiments showed a two-time-scale feature of the SO SST response to wind/SAM anomalies – a fast time-scale SST cooling response driven by the northward Ekman transport of surface waters and a slow time-scale SST warming response driven by the upwelling of warmer waters from below. Although a comprehensive study of such idealized experiments showed a very weak relationship between SAM and SST cooling on decadal time scales (Seviour et al., 2019), the appeal of a simple physical mechanism, the observed interannual modulation of SO SST by the SAM – and thus the Antarctic ozone hole – remains popular as a potential explanation of the multi-decadal cooling trends in the SO (Hartmann, 2022).

On the other hand, the causal relationship between SO SST trends and SAM/wind trends is at odds with several studies which have suggested that stratospheric ozone depletion causes surface *warming*, not cooling, on multi-decadal time scale. Unlike the idealized abrupt-forcing simulations that show a “fast” SO cooling response, GCM simulations with realistic transient or time-averaged ozone forcing robustly simulate a SO warming response along with Antarctic sea-ice melting (Sigmond & Fyfe, 2014; Bitz & Polvani, 2012; Smith et al., 2012; Landrum et al., 2017). Additionally, a recent study by Polvani et al. (2021) re-examined the relationship between the SAM and Antarctic sea-ice extent (SIE) in observations and GCMs. They found that the interannual SAM modulation of Antarctic SIE only explains a small fraction of the year-to-year SIE variability, and thus does not account for multi-decadal SIE trends. These studies collectively suggest that SAM variability, associated with the ozone hole, is unlikely to be the main driver of the observed long-term trends in SO SST and Antarctic SIE, contradicting the conclusion of the idealized modeling studies.

Motivated by these discrepancies in previous findings, we aim to address two questions in this study: (i) Can GCMs simulate the observed interannual relationship between the SAM and SO SST? (ii) To what extent does the interannual SAM modulation of SO SST contribute to the multi-decadal cooling trends in observations?

## 2 Interannual SAM modulation of Southern Ocean SST

In this section, we first repeat the analysis in Doddridge and Marshall (2017) (hereafter “DM2017”) and Polvani et al. (2021) to re-examine the interannual SAM-SST relationship in both observations and GCMs. By comparing the results between observations and models, we assess whether model biases in long-term SO SST trends stem in part from model biases in the short-term SAM-SST modulation.

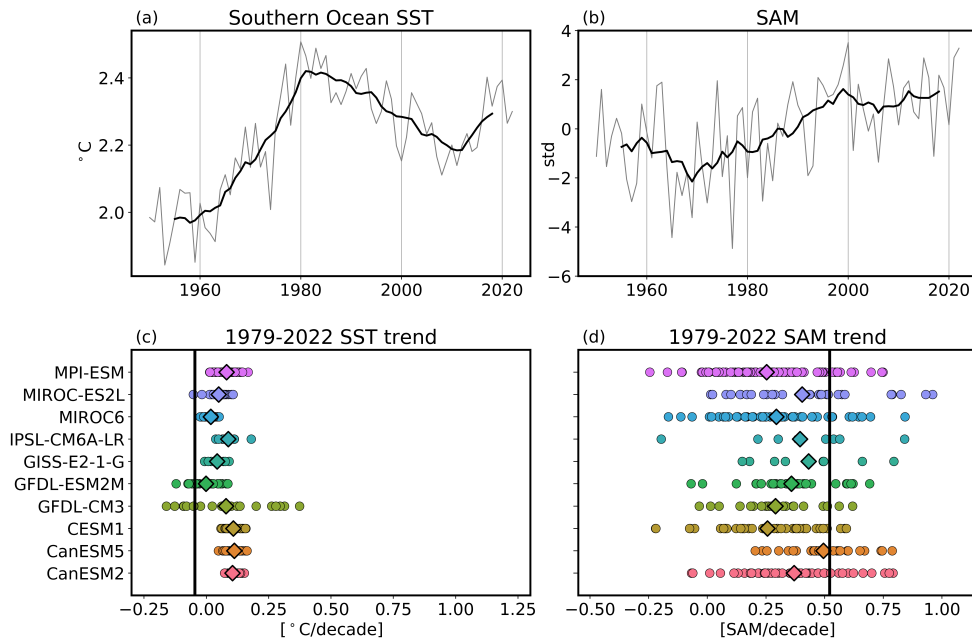


**Figure 1.** Observed and modeled Southern Ocean SST and SAM. (a – b) the observed annual-mean Southern Ocean SST and the DJF SAM index over 1950–2022. Black thicker lines denote 10-year running means. (c-d) the Southern Ocean SST trends and the SAM trend over 1979–2022 in observations (black line) and model large-ensembles. Circles denote each individual ensemble member; diamonds denote ensemble mean.

116

## 2.1 Data

117

118

119

120

121

122

123

124

125

126

127

128

For observations, we use SST from the NOAA Extended Reconstruction Sea Surface Temperature version 5 (ERSSTv5) dataset (Huang et al., 2017) and sea-level pressure (SLP) from the ERA5 Reanalysis dataset (Hersbach et al., 2020), both over the period of 1950–2022. For models, we use SST and SLP from 10 CMIP5 and CMIP6 models, including 5 models participated in multi-model large-ensemble project (Deser et al., 2020) and 5 CMIP6 models that have large ensembles (>10 members) of historical and SSP simulations. The main difference between the CMIP5 and CMIP6 ensembles is that the historical simulations extend to 2005 for CMIP5 but to 2014 for CMIP6. Thus, for the period up until 2022, we use RCP8.5 scenario for CMIP5 models and SSP245 or SSP370 scenario for CMIP6 models (see Table S1). Because forcing scenarios share similar trajectories early on in the 21st century, we expect this to cause little variation across model ensembles (Lehner et al., 2020).

129

130

131

132

133

134

135

136

137

We compute the SO SST index as the spatial average of the SST over  $50^{\circ}\text{S} - 70^{\circ}\text{S}$  following DM2017. The DJF seasonal-mean SAM index is computed as the difference between zonal-mean SLP at  $45^{\circ}\text{S}$  and  $60^{\circ}\text{S}$ , normalized by the 1971–2000 average, following G. J. Marshall (2003). We focus on DJF SAM because the recent SAM trend is only significant in DJF (Swart & Fyfe, 2012; Waugh et al., 2020) and has been robustly attributed to stratospheric ozone depletion (Polvani et al., 2011; Banerjee et al., 2020). For both observations and GCM outputs, we remove the linear trend in DJF SAM and monthly SO SST timeseries over the entire period 1950–2022, before we perform the regression analysis.

138

## 2.2 Results

139

140

141

142

143

144

145

146

147

148

149

150

151

152

153

We begin with SO SST regressions against DJF SAM in observations, to examine whether DJF SAM anomalies are followed by anomalous SO SST. That is, we regress the timeseries of the DJF SAM index onto SO SST in every calendar month, ranging from the same year’s December to next year’s November. Fig. 2 clearly shows that positive DJF SAM anomalies lead to SO SST cooling, which peaks in the same season (DJF) and gradually weakens in the following two seasons before eventually vanishing at the end of the year. This independently confirms the findings of DM2017, who showed that the SAM impact on SO SST (derived from a shorter time period of 1981–2017 in that study) is highly seasonal and does not persist over a year. Furthermore, our analysis reveals that the annually-averaged SST anomaly following a unit of positive SAM is only  $-0.05\text{ K}$  (Fig. 2a) and the portion of SST variance explained ( $r^2$ ) is merely 0.2 (Fig. 2b). Therefore, while positive SAM can indeed lead to SO SST cooling, we emphasize that this modulation occurs only on a seasonal timescale and can barely sustain at interannual or longer timescales. A similar result was reported by Polvani et al. (2021) for the DJF SAM modulation of Antarctic SIE.

154

155

156

157

158

159

Next, we repeat this regression analysis with model large ensembles. Perhaps surprisingly, models well reproduce the observed relationship between the DJF SAM and monthly SO SST (Fig. 2a, b grey lines), despite failing to simulate multi-decadal SO cooling (Fig. 1c). In fact, the multi-model mean regression even overestimates the maximum DJF SO SST cooling response and accounts for a higher SO SST variance (higher  $r^2$ ) (also see Fig. S1 and S2 for individual models).

160

161

162

163

164

165

166

To further investigate how the SAM modulation of SO SST impacts model-simulated long-term SST trends, we separate all model ensemble members (365 in total) into two groups: one consisting of all the members that simulate a negative trend of SO SST over 1979–2022 (35 members, blue lines in Fig. 2) and the other consisting of the rest of members (330 members, orange lines in Fig. 2). Although the ensemble members that can simulate the long-term SO cooling all produce a stronger SST cooling response to SAM, the members that fail to simulate the long-term cooling are also able to capture or even

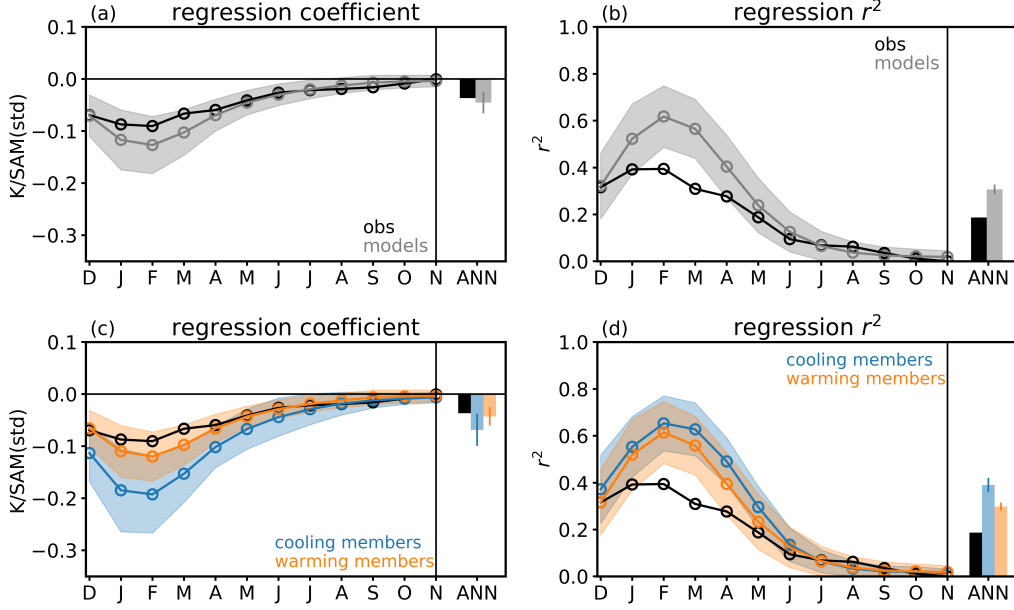


**Figure 2.** Regressions of monthly Southern Ocean SST (starting from DJF) onto same year’s DJF SAM. (a-c) regression coefficient; (b-d)  $r^2$  values of the regressions. Observations are shown in black, multi-model multi-ensemble means in grey, the ensemble members that simulate a negative SO SST trend over 1979–2022 (“cooling members”) in blue, and the members that simulate a positive SO SST trend (“warming members”) in orange. All shadings denote one standard deviation across ensemble members.

167 overestimate the observed SST response to SAM. These results suggest that correctly  
 168 simulating the seasonal-to-interannual SAM modulation of SO SST does not guarantee  
 169 the model’s performance on multi-decadal SO SST trends, implying that short-term and  
 170 long-term SST variability may be caused by different processes in models.

### 171 3 Low-frequency variability in the Southern Ocean

172 In the previous section, we have shown that in both observations and models the  
 173 SO SST cooling response to positive SAM anomalies only occurs in the same and fol-  
 174 lowing seasons. This raises a key question: Given the observed long-term SAM trend,  
 175 to what extent does the short-term SAM-SST relationship contribute to the observed  
 176 long-term SO cooling?

177 In the case of Antarctic SIE, Polvani et al. (2021) addressed this question by compar-  
 178 ing the actual SIE trend in observation with the estimate based on the SAM-SIE reg-  
 179 ression. They found that the long-term SAM-regressed SIE trend is much smaller than  
 180 the actual SIE trend, suggesting that the SAM is not the major driver of the observed  
 181 long-term SIE trend. We performed the same analysis for the SO SST and found a sim-  
 182 ilar result: the SAM-regressed annual-mean SO SST trend (1979–2022) is only 40% of  
 183 the actual SO SST trend. However, such an analysis using the zonal-mean SAM index  
 184 may overlook the spatial heterogeneity in the variability of winds and SST, and the re-  
 185 constructed SST trend may also be sensitive to the time period selected (an issue reported  
 186 by Polvani et al. 2021). Therefore, in this section, we revisit this question by employ-  
 187 ing a novel statistical method called low-frequency component analysis (LFCA; Wills et

188 al., 2018), to identify modes of low-frequency variability in observed zonal winds and the  
 189 SST changes associated with them.

### 190 3.1 LFCA method

191 LFCA (Wills et al., 2018) is a relatively new statistical technique – similar to the  
 192 conventional principal component analysis – to compute a linear combination of empir-  
 193 ical orthogonal functions (EOFs). LFCA maximizes the ratio of low-pass filtered vari-  
 194 ance to total variance, such that it isolates leading modes of low-frequency variability  
 195 and extracts physically-based modes in spatial-temporal signals in climate fields. It has  
 196 been applied to examine a wide range of climate quantities, including variability in global  
 197 SST anomalies (Wills et al., 2022), Atlantic ocean heat transport (Oldenburg et al., 2021),  
 198 and Arctic and Antarctic sea-ice concentration (Dörr et al., 2023; Bonan et al., 2023).

199 There are several advantages of using LFCA to investigate the relationship between  
 200 long-term SAM and SST. First, it helps separate low-frequency (decadal to multi-decadal)  
 201 and high-frequency (interannual) variability in SAM, allowing us to isolate the long-term  
 202 contribution of SAM to SST trends. Second, instead of directly using the simpler zonal-  
 203 mean SAM timeseries, we apply LFCA to the observed zonal winds at 850 hPa at each  
 204 latitude and longitude and find the timeseries associated with the leading mode of wind  
 205 variability. This gives us a more complete understanding of the relationship between winds  
 206 and SST as it accounts for spatial variability of winds and SST. This is important be-  
 207 cause several recent studies have pointed out the non-zonal feature of the observed SAM-  
 208 associated wind changes (Vaughn et al., 2020) and its zonally asymmetric impacts on SO  
 209 and remote SSTs (Dong, Armour, et al., 2022).

210 Our analysis uses the observed zonal winds at 850 hPa (U850) from the ERA5 Re-  
 211 analysis dataset (Hersbach et al., 2020). As with the SAM index analyzed in section 2,  
 212 we consider DJF U850 over 1950–2022. We apply LFCA to the observed U850 only over  
 213 40°S – 80°S, to avoid variability associated with tropical winds. Our LFCA uses a 15-  
 214 year cutoff low-pass filter to isolate low-frequency variability, and we retain the 5 lead-  
 215 ing EOFs, which account for 77% of the total U850 variability (we find that increasing  
 216 the number of EOFs does not lead to substantially more variance explained). The LFCA  
 217 results remain the same regardless we choose a low-pass filter of 10 year, 15 year or 20  
 218 year (compare Fig. S3 to Fig. 3).

### 219 3.2 LFCA results

220 First, let us consider the leading anomaly patterns (i.e., low-frequency patterns,  
 221 LFPs) and their associated timeseries (i.e., low-frequency components, LFCs) obtained  
 222 by applying LFCA to the observed DJF U850 over the Southern Ocean. The first 5 LFPs  
 223 and LFCs are shown in Fig. 3, in the left and right columns, respectively.

224 The leading mode (LFP1) features a SAM-like annular pattern of wind strength-  
 225 ening that has increased monotonically from 1970s to 2000s (see LFC1). This is well in  
 226 line with the SAM trend caused by ozone depletion (Banerjee et al., 2020). This mode  
 227 accounts for 58.3% of the low-frequency variance and has the highest signal-to-noise ra-  
 228 tio of 0.4. The next four modes exhibit mostly non-zonal patterns (LFP2-5), where wind  
 229 anomalies are confined to specific ocean sectors. The LFCs associated with LFP2 and  
 230 LFP3 have some decadal-to-multi-decadal variability, while the LFCs associated with  
 231 LFP4 and LFP5 are dominated by interannual variability, consistent with their low signal-  
 232 to-noise ratio.

233 Next, we examine the U850 trend pattern (1979–2022) associated with each mode  
 234 by projecting each LFC onto the corresponding LFP of U850 at each grid point over the  
 235 SO. Fig. S4 confirms that the total reconstruction based on the five LFPs (Fig. S4b) well  
 236 reproduces the observed U850 trend pattern (Fig. S4a), which is characterized by a strength-

237 ening of the westerlies at high latitudes in the Southern Ocean. Furthermore, the total  
 238 reconstructed trend pattern remains the same using either the leading five or three LFPs,  
 239 suggesting that LFP 1-3 are the major contributor to the total U850 trends over recent  
 240 decades.

### 241 3.3 Long-term relationship between SO SST and winds

242 Having established that the leading modes obtained by LFCA well reproduce the  
 243 observed U850 trend pattern, we next investigate the long-term relationship between U850  
 244 and SO SST by examining how each LFP and LFC influences SST across timescales.

245 First, we regress the observed DJF SST over the entire period (1950–2022) at each  
 246 grid box onto the LFC timeseries associated with the three leading wind LFPs, respec-  
 247 tively (Fig. 4 a-c). We focus on DJF SST as our earlier results suggest it is the season  
 248 when the SAM, through surface winds, has the strongest impact on SST. Consistent with  
 249 the SAM-SST regression result (Fig. 2), the wind LFC-SST regression also shows broad  
 250 SST cooling anomalies around Antarctica associated with positive LFC anomalies. How-  
 251 ever, it is interesting that the patterns of SST cooling response do not quite match the  
 252 wind anomaly patterns (compare Fig. 3 and Fig. 4): All three wind LFPs feature posi-  
 253 tive wind anomalies throughout the Southern Ocean (LFP1 even has stronger wind anoma-  
 254 lies in the Atlantic basin than in the Pacific basin), yet their SST cooling responses are  
 255 most significant in the Pacific basin. This mismatch in spatial patterns may give us a  
 256 first hint that the proposed mechanism linking surface winds to SO SST through Ekman  
 257 heat transport may not sufficiently explain the spatial patterns of wind-SST relation-  
 258 ship.

259 Second, we estimate the long-term SST trends over the period 1979–2022 based on  
 260 the above linear regression. Specifically, we multiply the regression between each LFC  
 261 and SST at each grid box with the corresponding LFC, and then take the linear trend  
 262 of the reconstructed SST timeseries at each grid box (Fig. 4). Although the LFC-based  
 263 SST trends also occur in the Pacific basin – consistent with observations – one imme-  
 264 diately sees that the magnitudes of wind-driven SST trends are much weaker than that  
 265 observed (cf. Fig. 4 middle row vs. Fig. 4g). Taking a spatial average over the Pacific  
 266 sector of the Southern Ocean where the observed SST cooling is strongest (150°E – 60°W,  
 267 50°S – 70°S), we obtain an SST trend of  $-0.98$  °C/decade from the observation, and SST  
 268 trends of  $-0.25$ ,  $-0.14$  and  $-0.02$  °C/decade from LFC1-3 regressions respectively, which  
 269 altogether account for less than half of the actual SST trend (Fig. 4i). To further illus-  
 270 trate the inability of winds to account for the time-evolution of SO SST, we plot the time-  
 271 series of DJF SO SST anomalies (relative to their climatology) for the observation and  
 272 for the estimates using LFC1-3 regressions (Fig. 4h). Although each of the LFCs con-  
 273 tributes to some SST variability, none of them can produce a multi-decadal SO SST vari-  
 274 ability as strong as the observed timeseries. Even the sum of all three LFC-regression-  
 275 based SO SST timeseries fails to explain the much larger multi-decadal trends in the ob-  
 276 served SO SST.

277 Furthermore, our SST trend estimates so far have been focused on DJF, in the same  
 278 season with wind anomalies, so as to capture the strongest wind impacts on SST. We  
 279 also repeated the analysis for annual-mean (instead of DJF only) SST (Fig. S5). The  
 280 annual-mean SST anomalies following a unit of DJF wind LFC changes are even weaker,  
 281 leading to almost negligible wind-driven annual-mean SST trends over recent decades,  
 282 i.e.,  $-0.16$  °C/decade over 1979–2022 from all three leading-mode regressions, compared  
 283 to  $-0.9$  °C/decade of the actual SST trend (Fig. S5j).

284 Thus, by projecting SO SST onto the leading modes of observed wind variability,  
 285 we find that although positive DJF wind anomalies can cause some SST cooling in the  
 286 same season, this modulation does not survive more than a few months, and the result-  
 287 ing wind-driven SST cooling is *too weak* to explain the large multi-decadal trend in the

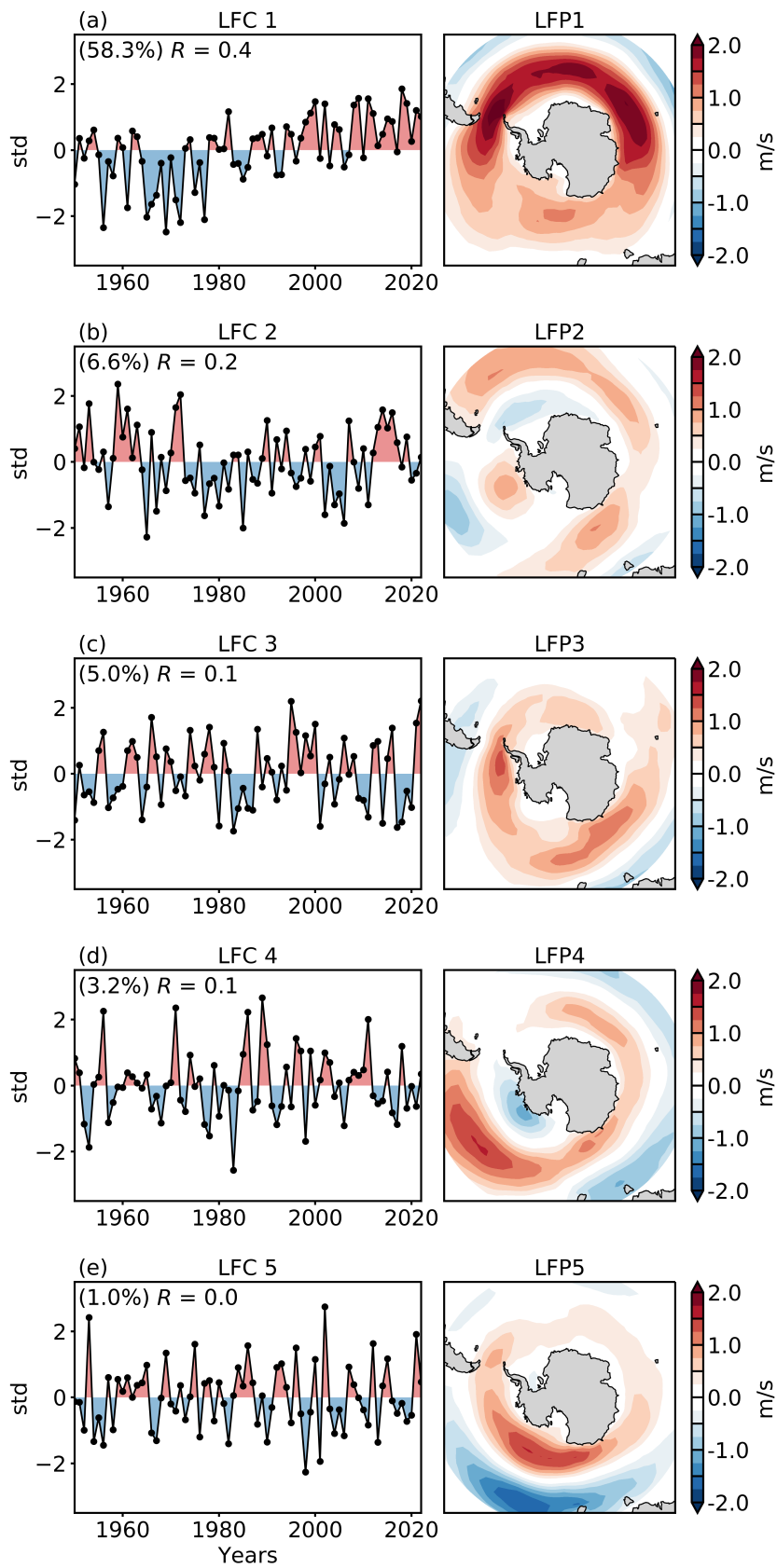


**Figure 3.** Low-frequency patterns (LFP; right column; unit: m/s) and their associated components (LFC; left column; unit: standard deviation) for the observed DJF U850 wind anomalies. Values in parentheses in the LFC panels denote the low-frequency variance explained by each mode.  $R$  values denote the ratio of low-frequency variance explained to the total variance, representing the signal-to-noise ratio.

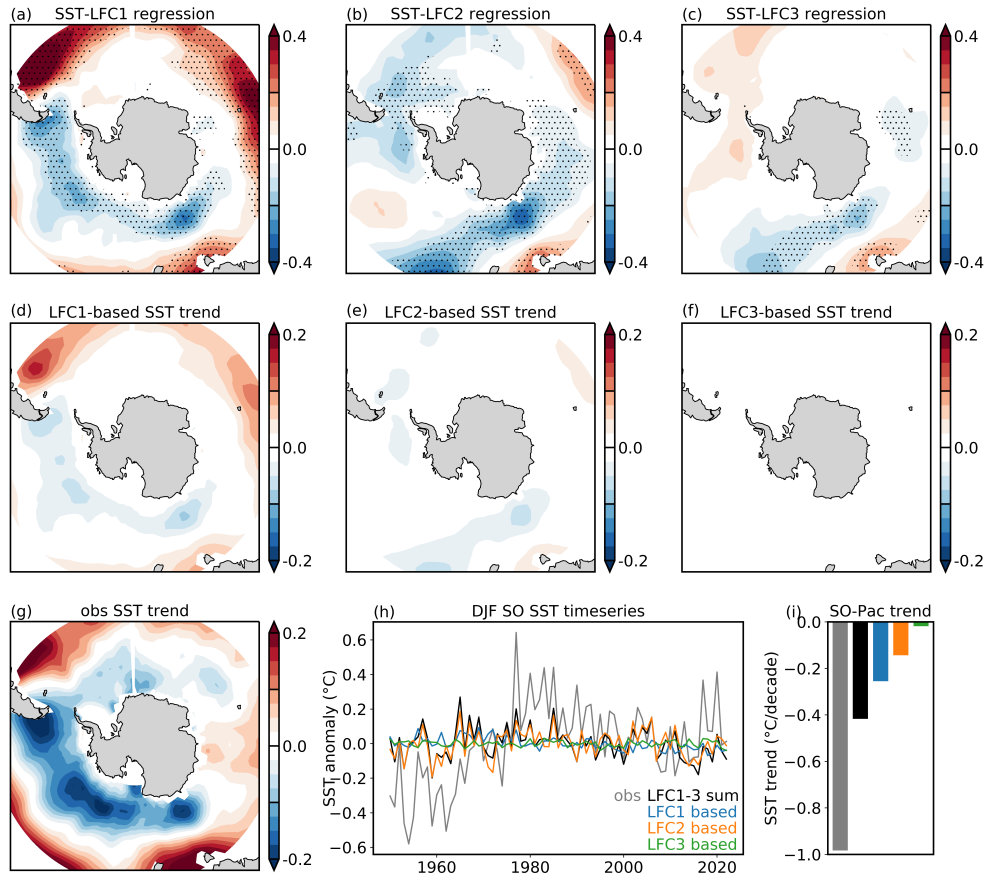


**Figure 4.** (a-c) DJF SST regression map onto LFC1-3 respectively (unit:  $^{\circ}\text{C}/\text{std}$ ). Stippling indicates where linear regression is statistically significant at 95% level. (d-g) DJF SST trend patterns over 1979–2022 ( $^{\circ}\text{C}/\text{decade}$ ) estimated from regressions with LFC 1-3 respectively and ERSSTv5. (i) Timeseries of SO SST anomalies relative to their climatology and (j) SST trends averaged over the Pacific sector over 1979–2022, from the observation (grey), the regressions with LFC1-3 respectively (colored), and all three leading LFCs (black).

288 observed Southern Ocean SST (Fig. 4). Hence, the recent wind strengthening over the  
 289 Southern Ocean is unlikely the key driver of the long-term Southern Ocean cooling.

## 290 4 Summary and Discussion

291 In this study, we have re-examined a previously proposed idea that positive SAM  
 292 anomalies in DJF, associated with a strengthening of the circumpolar westerlies, may  
 293 in part explain the observed Southern Ocean cooling (J. Marshall et al., 2014; Ferreira  
 294 et al., 2015; Doddridge & Marshall, 2017; Kostov et al., 2018; Hartmann, 2022). Using  
 295 GCM large-ensembles, we have found that models are able to capture the observed seasonal-  
 296 to-interannual modulation of SO SST by the SAM, regardless of whether they are able

297 to simulate the long-term SO cooling. Focusing on observations, we have shown that al-  
298 though positive SAM anomalies and positive zonal wind anomalies in DJF can lead to  
299 some SST cooling anomalies in the same season, this mechanism only operates for a few  
300 months and does not persist from year to year. These results suggest that the SAM mod-  
301 ulation of SO SST, via the strengthening of SO westerlies, is too weak to explain the ob-  
302 served multi-decadal Southern Ocean cooling.

303 One novel aspect of our study is that we used a low-frequency component analy-  
304 sis to isolate trends in SO zonal winds, rather than focusing on trends in the SAM. While  
305 the SAM index has been widely used as a metric to quantify zonal wind changes in the  
306 Southern Hemisphere, it only represents zonal-mean features and includes a wide range  
307 of variabilities from interannual to decadal timescales. Applying LFCA to the observed  
308 wind anomalies has allowed us to (1) obtain the timeseries (LFCs) of the leading modes  
309 of wind variability while retaining the spatial pattern of the wind anomalies, and (2) dis-  
310 entangle low-frequency from high-frequency variability.

311 It could be argued that the weak connection between long-term SAM and SST trends  
312 can be immediately deduced from the SAM and SST timeseries alone. A simple visual  
313 inspection of their smoothed timeseries (thick curves in Fig. 1a and b, respectively) suf-  
314 fices to note that the kinks in those curves do not match. The SST cooling starts after  
315 1980 and persists past 2010, whereas the positive SAM trend starts well before 1970 and  
316 stops after 2000, as a consequence of the Montreal Protocol (Banerjee et al., 2020). Build-  
317 ing on this, our new analysis, accounting for spatial-temporal variability, adds additional  
318 evidence corroborating the inability of the SAM and surface westerlies to explain the re-  
319 cent multi-decadal SO cooling.

320 Understanding the causes of the observed Southern Ocean cooling and biases in  
321 climate models remains a major challenge. By showing that the SAM-driven SST cool-  
322 ing is too weak to explain the long-term SO SST trends, our results point to a possibly  
323 limited role of stratospheric ozone depletion. This finding is also consistent with recent  
324 modeling evidence that nudging tropospheric wind anomalies around Antarctica towards  
325 observations in a GCM (CESM1) does not produce significant SO SST cooling over re-  
326 cent four decades (Blanchard-Wrigglesworth et al., 2021; Dong, Armour, et al., 2022).  
327 Thus, the impact of the Antarctic ozone hole on long-term SO SST via the SAM appears  
328 to be less robust than previously proposed. Even so, there is evidence that the ozone hole  
329 has caused remote climate impacts on lower latitudes, notably on subtropical precipi-  
330 tation (Kang et al., 2011; Gonzalez et al., 2014; Wu & Polvani, 2017). The Antarctic ozone  
331 hole, therefore, may have impacted SST in remote regions (e.g., the tropical Pacific), and  
332 those impacts could then have been communicated back to the Southern Ocean SST via  
333 atmospheric teleconnections (Ding et al., 2011; Meehl et al., 2016; Chung et al., 2022;  
334 Dong, Armour, et al., 2022). Such complex two-way teleconnections, however, remain  
335 largely unexplored.

336 Beyond potential remote impacts from the tropics, other local contributors to the  
337 recent SO cooling remain plausible, including freshwater input from Antarctic ice-sheet  
338 melt or more equatorward sea-ice melt (Purich et al., 2018; Bintanja et al., 2013; Rye  
339 et al., 2020; Dong, Pauling, et al., 2022; Haumann et al., 2020), and Southern Ocean nat-  
340 ural variability (Latif et al., 2013; Cabré et al., 2017; Zhang et al., 2019). Whether the  
341 recent SO cooling was driven by historical forcings or simply reflects natural variabil-  
342 ity has important implications for SST trends in the near future. Accurately constrain-  
343 ing future projections of Antarctic climate change thus requires a better understanding  
344 of the causes of the recent multi-decadal Southern Ocean SST trends.

## 345 **Acknowledgments**

346 YD was supported by the NOAA Climate and Global Change Postdoctoral Fellowship  
347 Program, administered by UCAR's Cooperative Programs for the Advancement of Earth

348 System Science (CPAESS) under award NA210AR4310383. DBB was supported by the  
 349 National Science Foundation (NSF) Graduate Research Fellowship Program (NSF Grant  
 350 DGE-1745301). LMP is grateful to the US NSF for their continued support, under award  
 351 #1914569.

## 352 Data Availability Statement

353 ERSSTv5 SST data is available at <https://psl.noaa.gov/data/gridded/data.noaa.ersst.v5.html>.  
 354 ERA5 reanalysis SLP and U850 data is available from the Copernicus Climate Service  
 355 at <https://cds.climate.copernicus.eu/>. CMIP5 and CMIP6 model multi-model large en-  
 356 sembles are available via the NCAR Climate Data Gateway and via the ESGF archive  
 357 at: <https://esgf-node.llnl.gov/search/cmip6/>.

## 358 References

- 359 Armour, K. C., Marshall, J., Scott, J. R., Donohoe, A., & Newsom, E. R. (2016).  
 360 Southern Ocean warming delayed by circumpolar upwelling and equatorward  
 361 transport. *Nature Geoscience*, *9*(7), 549–554.
- 362 Banerjee, A., Fyfe, J. C., Polvani, L. M., Waugh, D., & Chang, K.-L. (2020). A  
 363 pause in Southern Hemisphere circulation trends due to the Montreal Protocol.  
 364 *Nature*, *579*(7800), 544–548.
- 365 Bintanja, R., van Oldenborgh, G. J., Drijfhout, S., Wouters, B., & Katsman, C.  
 366 (2013). Important role for ocean warming and increased ice-shelf melt in  
 367 Antarctic sea-ice expansion. *Nature Geoscience*, *6*(5), 376–379.
- 368 Bitz, C., & Polvani, L. M. (2012). Antarctic climate response to stratospheric ozone  
 369 depletion in a fine resolution ocean climate model. *Geophysical Research Let-  
 370 ters*, *39*(20).
- 371 Blanchard-Wrigglesworth, E., Roach, L. A., Donohoe, A., & Ding, Q. (2021). Impact  
 372 of winds and Southern Ocean SSTs on Antarctic sea ice trends and variability.  
 373 *Journal of Climate*, *34*(3), 949–965.
- 374 Bonan, D. B., Dörr, J., Wills, R. C., Thompson, A. F., & Årthun, M. (2023).  
 375 Sources of low-frequency variability in observed Antarctic sea ice. *EGU sphere*,  
 376 *2023*, 1–28.
- 377 Cabré, A., Marinov, I., & Gnanadesikan, A. (2017). Global atmospheric tele-  
 378 connections and multidecadal climate oscillations driven by Southern Ocean  
 379 convection. *Journal of Climate*, *30*(20), 8107–8126.
- 380 Chung, E.-S., Kim, S.-J., Timmermann, A., Ha, K.-J., Lee, S.-K., Stuecker, M. F., et  
 381 al. (2022). Antarctic sea-ice expansion and Southern Ocean cooling linked to  
 382 tropical variability. *Nature Climate Change*, *12*(5), 461–468.
- 383 De Lavergne, C., Palter, J. B., Galbraith, E. D., Bernardello, R., & Marinov, I.  
 384 (2014). Cessation of deep convection in the open Southern Ocean under an-  
 385 thropogenic climate change. *Nature Climate Change*, *4*(4), 278–282.
- 386 Deser, C., Lehner, F., Rodgers, K. B., Ault, T., Delworth, T. L., DiNezio, P. N.,  
 387 ... others (2020). Insights from Earth system model initial-condition large  
 388 ensembles and future prospects. *Nature Climate Change*, *10*(4), 277–286.
- 389 Ding, Q., Steig, E. J., Battisti, D. S., & Küttel, M. (2011). Winter warming in West  
 390 Antarctica caused by central tropical Pacific warming. *Nature Geoscience*,  
 391 *4*(6), 398–403.
- 392 Doddridge, E. W., & Marshall, J. (2017). Modulation of the seasonal cycle of  
 393 Antarctic sea ice extent related to the Southern Annular Mode. *Geophysical  
 394 Research Letters*, *44*(19), 9761–9768.
- 395 Dong, Y., Armour, K. C., Battisti, D. S., & Blanchard-Wrigglesworth, E. (2022).  
 396 Two-way teleconnections between the Southern Ocean and the tropical Pacific  
 397 via a dynamic feedback. *Journal of Climate*, 1–37.

- 398 Dong, Y., Pauling, A. G., Sadai, S., & Armour, K. C. (2022). Antarctic ice-sheet  
399 meltwater reduces transient warming and climate sensitivity through the sea-  
400 surface temperature pattern effect. *Geophysical Research Letters*, *49*(24),  
401 e2022GL101249.
- 402 Dörr, J. S., Bonan, D. B., Árrthun, M., Svendsen, L., & Wills, R. C. (2023). Forced  
403 and internal components of observed Arctic sea-ice changes. *The Cryosphere*  
404 *Discussions*, 1–27.
- 405 Fan, T., Deser, C., & Schneider, D. P. (2014). Recent Antarctic sea ice trends in  
406 the context of Southern Ocean surface climate variations since 1950. *Geophys-  
407 ical Research Letters*, *41*(7), 2419–2426.
- 408 Ferreira, D., Marshall, J., Bitz, C. M., Solomon, S., & Plumb, A. (2015). Antarc-  
409 tic Ocean and sea ice response to ozone depletion: A two-time-scale problem.  
410 *Journal of Climate*, *28*(3), 1206–1226.
- 411 Gonzalez, P. L., Polvani, L. M., Seager, R., & Correa, G. J. (2014). Stratospheric  
412 ozone depletion: a key driver of recent precipitation trends in South Eastern  
413 South America. *Climate Dynamics*, *42*, 1775–1792.
- 414 Gupta, A. S., & England, M. H. (2006). Coupled ocean–atmosphere–ice response  
415 to variations in the southern annular mode. *Journal of Climate*, *19*(18), 4457–  
416 4486.
- 417 Hall, A., & Visbeck, M. (2002). Synchronous variability in the Southern Hemi-  
418 sphere atmosphere, sea ice, and ocean resulting from the annular mode. *Jour-  
419 nal of Climate*, *15*(21), 3043–3057.
- 420 Hartmann, D. L. (2022). The Antarctic ozone hole and the pattern effect on cli-  
421 mate sensitivity. *Proceedings of the National Academy of Sciences*, *119*(35),  
422 e2207889119.
- 423 Haumann, F. A., Gruber, N., & Münnich, M. (2020). Sea-ice induced southern  
424 ocean subsurface warming and surface cooling in a warming climate. *AGU Ad-  
425 vances*, *1*(2), e2019AV000132.
- 426 Hersbach, H., Bell, B., Berrisford, P., Hirahara, S., Horányi, A., Muñoz-Sabater, J.,  
427 ... others (2020). The ERA5 global reanalysis. *Quarterly Journal of the Royal*  
428 *Meteorological Society*, *146*(730), 1999–2049.
- 429 Huang, B., Thorne, P. W., Banzon, V. F., Boyer, T., Chepurin, G., Lawrimore,  
430 J. H., ... Zhang, H.-M. (2017). Extended reconstructed sea surface tem-  
431 perature, version 5 (ERSSTv5): upgrades, validations, and intercomparisons.  
432 *Journal of Climate*, *30*(20), 8179–8205.
- 433 Hwang, Y.-T., Xie, S.-P., Deser, C., & Kang, S. M. (2017). Connecting tropical cli-  
434 mate change with southern ocean heat uptake. *Geophysical Research Letters*,  
435 *44*(18), 9449–9457.
- 436 Kang, S. M., Polvani, L. M., Fyfe, J., & Sigmond, M. (2011). Impact of polar ozone  
437 depletion on subtropical precipitation. *Science*, *332*(6032), 951–954.
- 438 Kang, S. M., Xie, S.-P., Shin, Y., Kim, H., Hwang, Y.-T., Stuecker, M. F., et al.  
439 (2020). Walker circulation response to extratropical radiative forcing. *Science*  
440 *advances*, *6*(47), eabd3021.
- 441 Kang, S. M., Yu, Y., Deser, C., Zhang, X., Kang, I.-S., Lee, S.-S., ... Ceppi, P.  
442 (2023). Global impacts of recent Southern Ocean cooling. *Proceedings of the*  
443 *National Academy of Sciences*, *120*(30), e2300881120.
- 444 Kim, H., Kang, S. M., Kay, J. E., & Xie, S.-P. (2022). Subtropical clouds key to  
445 Southern Ocean teleconnections to the tropical pacific. *Proceedings of the Na-  
446 tional Academy of Sciences*, *119*(34), e2200514119.
- 447 Kostov, Y., Ferreira, D., Armour, K. C., & Marshall, J. (2018). Contributions of  
448 greenhouse gas forcing and the Southern Annular Mode to historical South-  
449 ern Ocean surface temperature trends. *Geophysical Research Letters*, *45*(2),  
450 1086–1097.
- 451 Landrum, L. L., Holland, M. M., Raphael, M. N., & Polvani, L. M. (2017). Strato-  
452 spheric ozone depletion: An unlikely driver of the regional trends in antarctic

- 453 sea ice in austral fall in the late twentieth century. *Geophysical Research*  
 454 *Letters*, *44*(21), 11–062.
- 455 Latif, M., Martin, T., & Park, W. (2013). Southern Ocean sector centennial climate  
 456 variability and recent decadal trends. *Journal of Climate*, *26*(19), 7767–7782.
- 457 Lefebvre, W., Goosse, H., Timmermann, R., & Fichefet, T. (2004). Influence of the  
 458 Southern Annular Mode on the sea ice–ocean system. *Journal of Geophysical*  
 459 *Research: Oceans*, *109*(C9).
- 460 Lehner, F., Deser, C., Maher, N., Marotzke, J., Fischer, E. M., Brunner, L., ...  
 461 Hawkins, E. (2020). Partitioning climate projection uncertainty with multiple  
 462 large ensembles and CMIP5/6. *Earth System Dynamics*, *11*(2), 491–508.
- 463 Marshall, G. J. (2003). Trends in the Southern Annular Mode from observations and  
 464 reanalyses. *Journal of climate*, *16*(24), 4134–4143.
- 465 Marshall, J., Armour, K. C., Scott, J. R., Kostov, Y., Hausmann, U., Ferreira, D.,  
 466 ... Bitz, C. M. (2014). The ocean’s role in polar climate change: asymmetric  
 467 Arctic and Antarctic responses to greenhouse gas and ozone forcing. *Philo-*  
 468 *sophical Transactions of the Royal Society A: Mathematical, Physical and*  
 469 *Engineering Sciences*, *372*(2019), 20130040.
- 470 Meehl, G. A., Arblaster, J. M., Bitz, C. M., Chung, C. T., & Teng, H. (2016).  
 471 Antarctic sea-ice expansion between 2000 and 2014 driven by tropical Pacific  
 472 decadal climate variability. *Nature Geoscience*, *9*(8), 590–595.
- 473 Oldenburg, D., Wills, R. C., Armour, K. C., Thompson, L., & Jackson, L. C. (2021).  
 474 Mechanisms of low-frequency variability in North Atlantic Ocean heat trans-  
 475 port and AMOC. *Journal of Climate*, *34*(12), 4733–4755.
- 476 Parkinson, C. L. (2019). A 40-y record reveals gradual Antarctic sea ice increases  
 477 followed by decreases at rates far exceeding the rates seen in the Arctic. *Pro-*  
 478 *ceedings of the National Academy of Sciences*, *116*(29), 14414–14423.
- 479 Pauling, A. G., Bitz, C. M., Smith, I. J., & Langhorne, P. J. (2016). The response  
 480 of the Southern Ocean and Antarctic sea ice to freshwater from ice shelves in  
 481 an Earth system model. *Journal of Climate*, *29*(5), 1655–1672.
- 482 Polvani, L. M., Banerjee, A., Chemke, R., Doddridge, E., Ferreira, D., Gnanade-  
 483 sikan, A., ... others (2021). Interannual sam modulation of antarctic sea ice  
 484 extent does not account for its long-term trends, pointing to a limited role for  
 485 ozone depletion. *Geophysical Research Letters*, *48*(21), e2021GL094871.
- 486 Polvani, L. M., & Smith, K. L. (2013). Can natural variability explain observed  
 487 Antarctic sea ice trends? New modeling evidence from CMIP5. *Geophysical*  
 488 *Research Letters*, *40*(12), 3195–3199.
- 489 Polvani, L. M., Waugh, D. W., Correa, G. J., & Son, S.-W. (2011). Stratospheric  
 490 ozone depletion: The main driver of twentieth-century atmospheric circulation  
 491 changes in the Southern Hemisphere. *Journal of Climate*, *24*(3), 795–812.
- 492 Previdi, M., & Polvani, L. M. (2014). Climate system response to stratospheric  
 493 ozone depletion and recovery. *Quarterly Journal of the Royal Meteorological*  
 494 *Society*, *140*(685), 2401–2419.
- 495 Purich, A., & England, M. H. (2023). Projected impacts of Antarctic meltwater  
 496 anomalies over the twenty-first century. *Journal of Climate*, *36*(8), 2703–2719.
- 497 Purich, A., England, M. H., Cai, W., Sullivan, A., & Durack, P. J. (2018). Impacts  
 498 of broad-scale surface freshening of the Southern Ocean in a coupled climate  
 499 model. *Journal of Climate*, *31*(7), 2613–2632.
- 500 Roach, L. A., Dörr, J., Holmes, C. R., Massonnet, F., Blockley, E. W., Notz, D., ...  
 501 others (2020). Antarctic sea ice area in CMIP6. *Geophysical Research Letters*,  
 502 *47*(9), e2019GL086729.
- 503 Rye, C. D., Marshall, J., Kelley, M., Russell, G., Nazarenko, L. S., Kostov, Y., ...  
 504 Hansen, J. (2020). Antarctic glacial melt as a driver of recent Southern Ocean  
 505 climate trends. *Geophysical Research Letters*, *47*(11), e2019GL086892.
- 506 Seviour, W. J. M., Codron, F., Doddridge, E. W., Ferreira, D., Gnanadesikan, A.,  
 507 Kelley, M., ... others (2019). The southern ocean sea surface temperature

- 508 response to ozone depletion: A multimodel comparison. *Journal of Climate*,  
509 32(16), 5107–5121.
- 510 Seviour, W. J. M., Gnanadesikan, A., & Waugh, D. W. (2016). The transient re-  
511 sponse of the Southern Ocean to stratospheric ozone depletion. *Journal of Cli-  
512 mate*, 29(20), 7383–7396.
- 513 Sigmond, M., & Fyfe, J. C. (2014). The Antarctic sea ice response to the ozone hole  
514 in climate models. *Journal of Climate*, 27(3), 1336–1342.
- 515 Smith, K. L., Polvani, L. M., & Marsh, D. R. (2012). Mitigation of 21st century  
516 Antarctic sea ice loss by stratospheric ozone recovery. *Geophysical Research  
517 Letters*, 39(20).
- 518 Swart, N., & Fyfe, J. C. (2012). Observed and simulated changes in the South-  
519 ern Hemisphere surface westerly wind-stress. *Geophysical Research Letters*,  
520 39(16).
- 521 Thompson, D. W., & Solomon, S. (2002). Interpretation of recent Southern Hemi-  
522 sphere climate change. *Science*, 296(5569), 895–899.
- 523 Waugh, D. W., Banerjee, A., Fyfe, J. C., & Polvani, L. M. (2020). Contrasting  
524 recent trends in Southern Hemisphere Westerlies across different ocean basins.  
525 *Geophysical Research Letters*, 47(18), e2020GL088890.
- 526 Wills, R. C., Dong, Y., Proistosescu, C., Armour, K. C., & Battisti, D. S. (2022).  
527 Systematic climate model biases in the large-scale patterns of recent sea-  
528 surface temperature and sea-level pressure change. *Geophysical Research  
529 Letters*, 49(17), e2022GL100011.
- 530 Wills, R. C., Schneider, T., Wallace, J. M., Battisti, D. S., & Hartmann, D. L.  
531 (2018). Disentangling global warming, multidecadal variability, and el niño in  
532 Pacific temperatures. *Geophysical Research Letters*, 45(5), 2487–2496.
- 533 Wu, Y., & Polvani, L. M. (2017). Recent trends in extreme precipitation and tem-  
534 perature over southeastern South America: The dominant role of stratospheric  
535 ozone depletion in the CESM Large Ensemble. *Journal of Climate*, 30(16),  
536 6433–6441.
- 537 Zhang, L., Delworth, T. L., Cooke, W., & Yang, X. (2019). Natural variability of  
538 Southern Ocean convection as a driver of observed climate trends. *Nature Cli-  
539 mate Change*, 9(1), 59–65.

# Supporting Information for “Recent multi-decadal Southern Ocean surface cooling unlikely caused by Southern Annular Mode trends”

Yue Dong<sup>1,2</sup>, Lorenzo M. Polvani<sup>1,3</sup>, David B. Bonan<sup>4</sup>

<sup>1</sup>Lamont-Doherty Earth Observatory, Columbia University, Palisades, NY, USA

<sup>2</sup>Cooperative Programs for the Advancement of Earth System Science, University Corporation for Atmospheric Research, Boulder,  
CO, USA

<sup>3</sup>Department of Applied Physics and Applied Mathematics, Columbia University, New York, NY, USA

<sup>4</sup>Environmental Science and Engineering, California Institute of Technology, Pasadena, CA, USA

## Contents of this file

1. Table S1
2. Figures S1 - S5

---

Corresponding author: Yue Dong, [yd2644@columbia.edu](mailto:yd2644@columbia.edu)

August 29, 2023, 2:16am

**Table S1.** Model large-ensemble simulations used in this study

model	simulation	ensemble number
CanESM2	Historical, rcp8.5	50
CESM1	Historical, rcp8.5	40
GFDL-CM3	Historical, rcp8.5	20
GFDL-ESM2M	Historical, rcp8.5	30
MPI-ESM	Historical, rcp8.5	100
CanESM5	Historical, ssp245	25
GISS-E2-1-G	Historical, ssp370	10
IPSL-CM6A-LR	Historical, ssp370	10
MIROC6	Historical, ssp245	50
MIROC-ES2L	Historical, ssp245	30

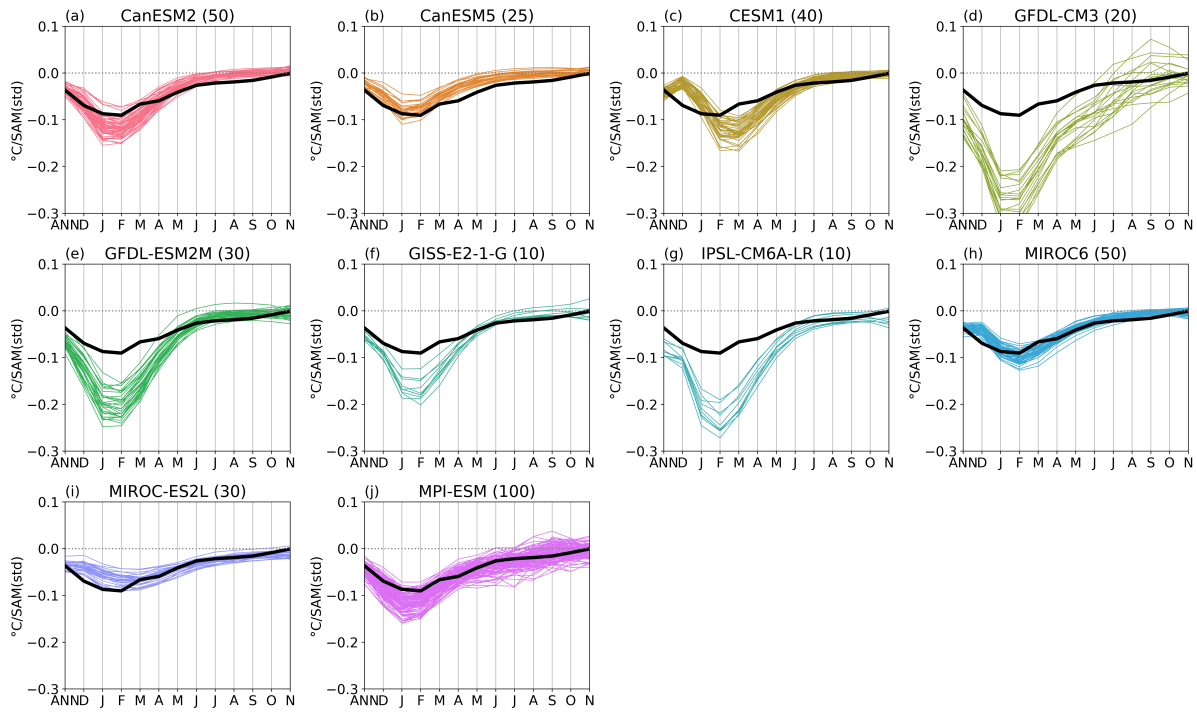


**Figure S1.** (a) Coefficients of monthly SST regressions onto DJF SAM for each individual model large-ensemble. Numbers in the title for each panel denotes the total number of ensemble members of the model.

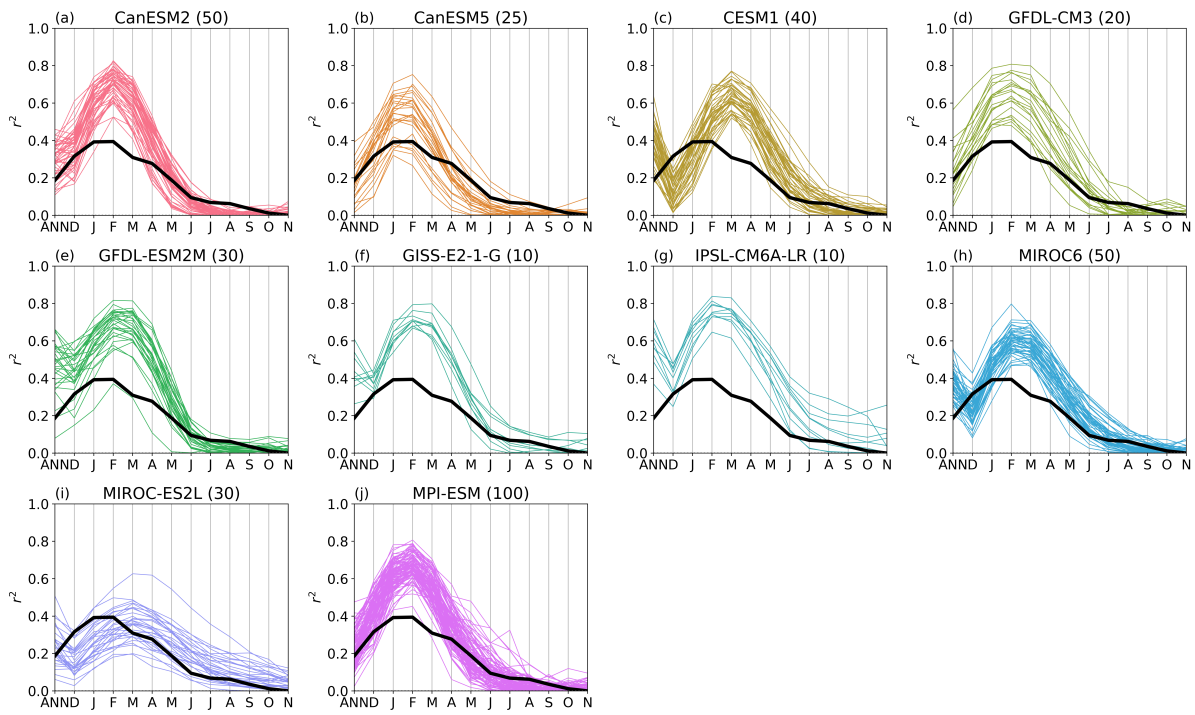


**Figure S2.** Same as Fig. S1, except for regression  $r^2$ .

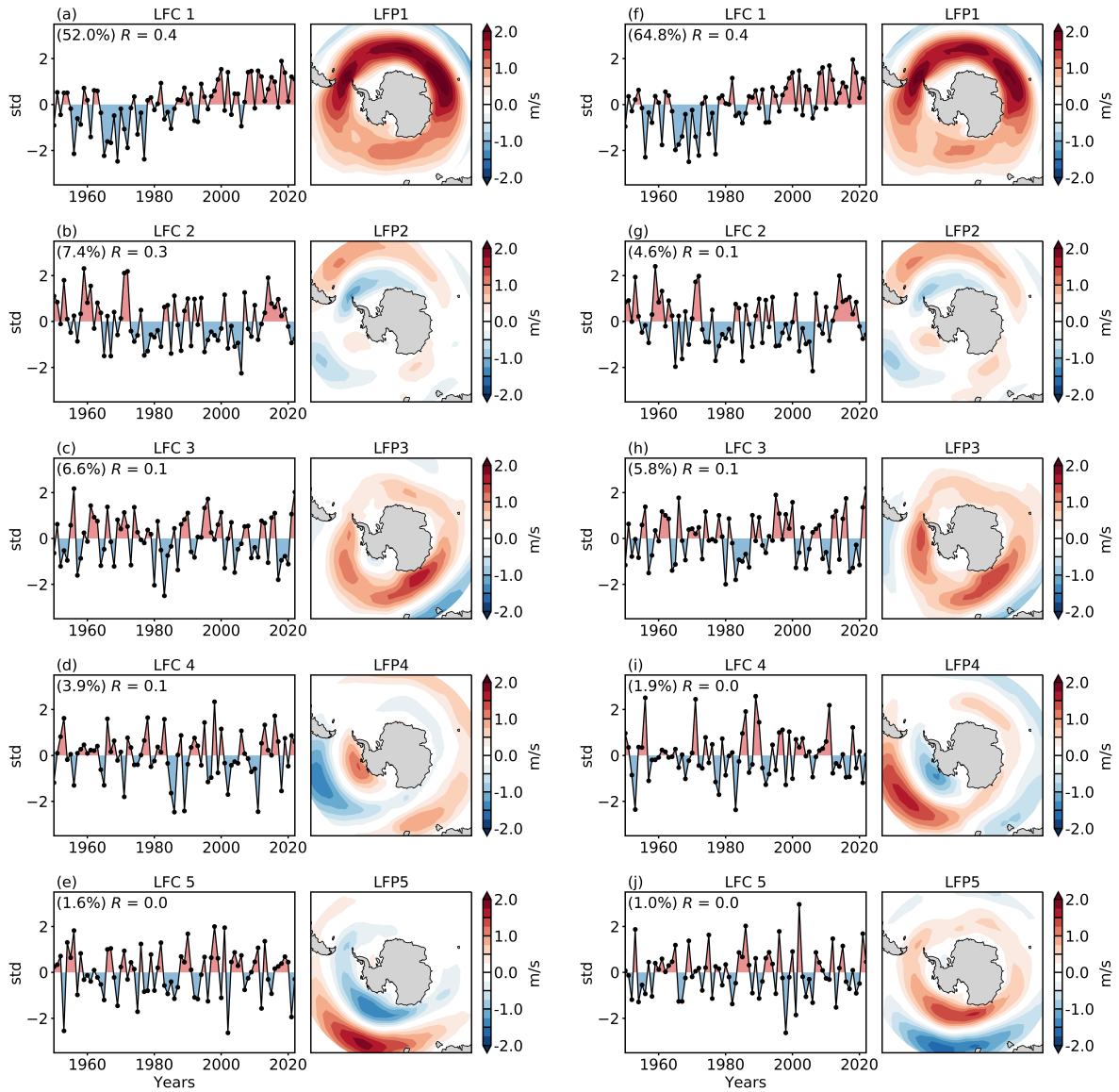


**Figure S3.** LFP and LFC results obtained using a cutoff of 10-year (left, a-e) or 20 year (right, f-j)

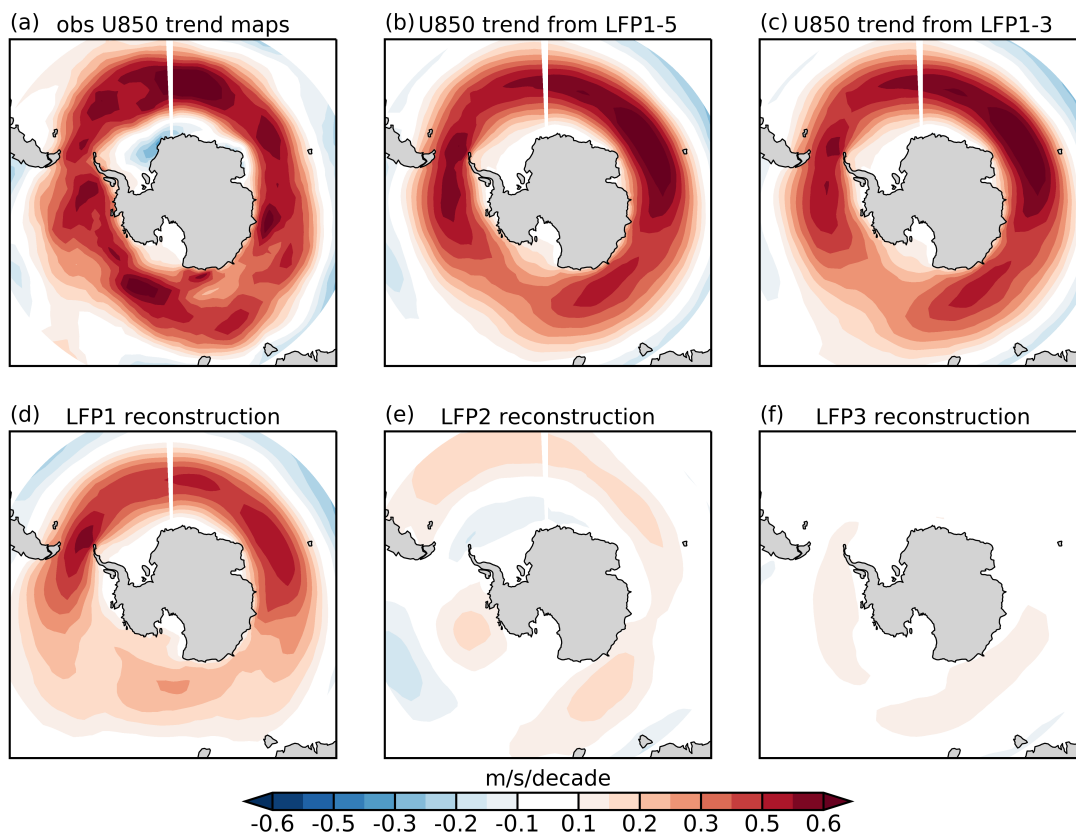


**Figure S4.** DJF U850 trend patterns over 1979-2022 (m/s/decade) from (a) ERA5 Reanalysis, (b, c) the reconstruction using all five LFPs or the leading three LFPs, and (d-f) the reconstructions using LFP 1-3, respectively.

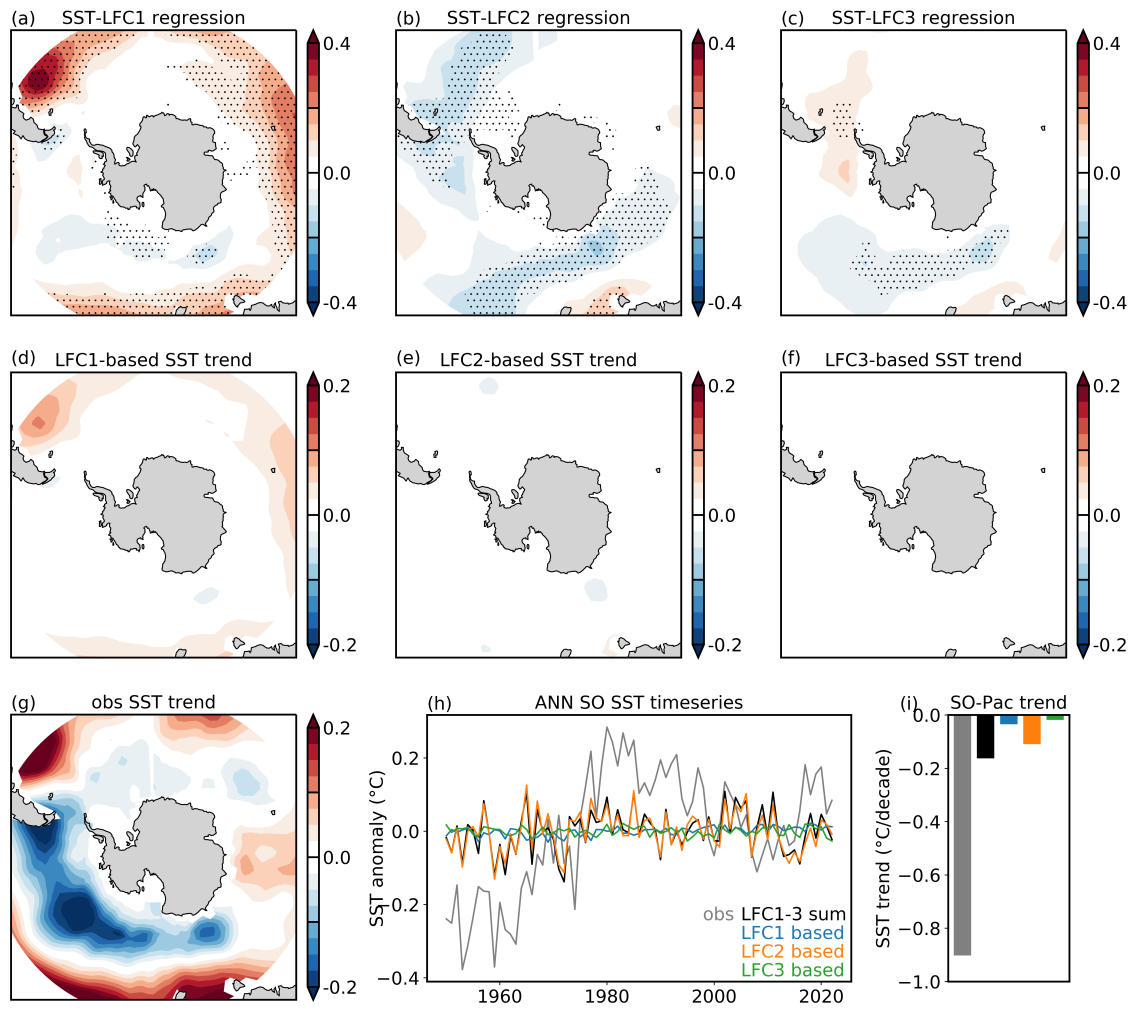


**Figure S5.** Same as Fig. 4, except for annual-mean SST regressions and trends.